A Theory for Strong, Long-Lived Squall Lines

RICHARD ROTUNNO, JOSEPH B. KLEMP AND MORRIS L. WEISMAN

National Center for Atmospheric Research, Boulder, Colorado*

(Manuscript received 27 February 1987, in final form 7 September 1987)

ABSTRACT

We study herein the mechanics of long-lived, line-oriented, precipitating cumulus convection (squall lines) using two- and three-dimensional numerical models of moist convection. These models, used in juxtaposition, enable us to address the important theoretical issue of whether a squall line is a system of special, long-lived cells, or whether it is a long-lived system of ordinary, short-lived cells. Our review of the observational literature indicates that the latter is the most consistent paradigm for the vast majority of cases, but, on occasion, a squall line may be composed of essentially steady, supercell thunderstorms. The numerical experiments presented herein show that either type of squall line may develop from an initial line-like disturbance depending on the magnitude and orientation of the environmental shear with respect to the line. With shallow shear, oriented perpendicular to the line, a long-lived line evolves containing individually short-lived cells. Our analysis of this type of simulated squall line suggests that the interaction of a storm cell's cold surface outflow with the low-level shear produces much-deeper and less-inhibited lifting than is possible without the low-level shear, making it easier for new cells to form and grow as old cells decay. Through intercomparsion of two- and three-dimensional squall-line simulations, we conclude that the essential physics of this type of squall line is contained in the two-dimensional framework. We argue that these results describe the physics of both midlatitude and tropical squall lines. Under conditions of deep strong shear at an angle to the supposed line, a line of supercells develops in which their respective three-dimensional circulations do not interfere with one another.

1. Introduction

A squall line is defined operationally as any line or narrow band of active thunderstorms (*Glossary of Meteorology*). Moreover, squall lines are generally observed to last several hours. These two basic features sharply distinquish the squall line from the more commonly observed mode of precipitating cumulus convection in which rain showers are widely scattered and intermittent. In a forthcoming paper, we report on a series of numerical experiments using the Klemp–Wilhelmson, three-dimensional cloud model, conducted under a wide variety of environmental conditions, that identify certain favorable conditions for long-lived, line-oriented convection. Herein we distill from these experiments, and past work in general, the essential mechanisms responsible for these favorable conditions, and show how this knowledge advances the general understanding of observed squall lines.

There are two distinct premises on which investigations into the nature of squall lines have been based. On the one hand, squall-line cumulonimbi are viewed as essentially different from ordinary cumulonimbi in that they may be more prone to having a steady structure. On the other hand, it is supposed that there is nothing particularly special about squall-line thunderstorms, only that they occur in concert along a line. Moncrieff (1978) makes this important distinction by referring to the study of *cell* and *system* dynamics, respectively.

One of the basic findings of the Thunderstorm Project (Byers and Braham, 1949, p. 19) was that a thunderstorm cell has a life cycle over which the cell updraft will yield to a downdraft induced by the accumulation of rain within the updraft and, for this reason, a thunderstorm cell is naturally short-lived (roughly 30–60 min; Fig. 1). Newton (1950) viewed the squall line as a *system* of convective updrafts and downdrafts aligned perpendicularly to the shear. He held that this ensemble of drafts acts to reduce the shear within the convective system and this, in turn, sets up a pattern of convergence and divergence which acts to produce new cells on the downshear and suppress old cells on the upshear side of the squall line (Fig. 2).

Ludlam (1963) developed the idea that a strong updraft tends to cant *against* the wind shear, allowing the updraft to unload its rain upshear, and permitting the updraft and downdraft circulations to continue indefinitely (Fig. 3). A collection of such long-lived cells, arranged along a straight line, would thus account for the squall line. Newton's (1966) later view was closer to Ludlam's single-*cell* concept as he focused on the nature of convective updrafts in shear. The schematic

* The National Center for Atmospheric Research is sponsored by the National Science Foundation.

Corresponding author address: Dr. Richard Rotunno, NCAR, P.O. Box 3000, Boulder, CO 80307-3000.

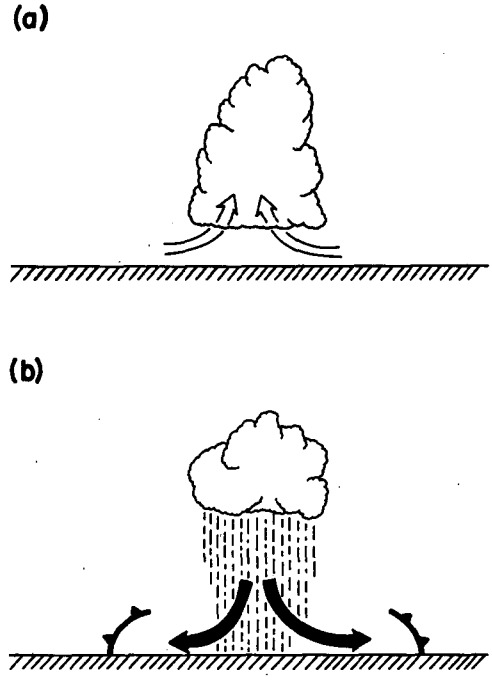

FIG. 1. Schematic illustration of the life cycle of an ordinary thunderstorm cell in which the (a) initial updraft, yields to a (b) downdraft produced by the accumulation of rain within the updraft. (Adapted from Figs. 17–18 of Byers and Braham, 1949.)

diagrams of Newton (1966) and Ludlam (1963) (see Fig. 3, hereinafter referred to as the Ludlam-Newton model) strongly suggested that such a steady two-dimensional *cell* is the basic building block of the squall line.

Two-dimensional numerical models of moist convection were developed in the early seventies (see the review by Lilly, 1979). Acting on the idea that wind shear directed normal to the line could permit a steady cell, the modelers tried to replicate the Ludlam–Newton observational model in their numerical simulations. Contrary to expectation, the two-dimensional simulations did not replicate that model, and further, did not reach *any* steady state in deep shear. The failure of the two-dimensional models to produce an intense, long-lived cell was generally thought to be due to the inherent three-dimensionality of cumulonimbus clouds (Lilly, 1979, p. 131). Three-dimensional models of moist convection showed later that essentially steady (often lasting for more than 2 h), three-dimensional, isolated supercells (Browning, 1964) could be simulated (e.g., see Klemp and Wilhelmson, 1978a).

By the end of the seventies, the modeling and observational studies had reached a dilemma; two-dimensional models failed to produce long-lived systems in deep shear, in apparent contradiction with the Ludlam–Newton observational model. One possible reconciliation is that Ludlam (1963) based his steady, two-dimensional model on the Browning and Ludlam (1962) analysis of a single thunderstorm, which in retrospect appears to have been a three-dimensional supercell. Thus a revised version of the Ludlam–Newton model might describe the squall line as a collection of supercells. Lilly (1979, p. 156) conjectured that a line of supercells could constitute a steady squall line if they aligned at an angle to the shear in such a way that their respective circulations did not interfere (see Fig. 4). Lilly (p. 155) and Moncrieff (1978, p. 565) suggested that the three-dimensional squall-line simulation of Moncrieff and Miller (1976) contained supercell-like circulations which allowed their system to be long lived. Thus, these observations and model results were apparently reconciled.

However, most squall lines are not composed of supercell thunderstorms (Bluestein and Jain, 1985) and the question remained whether, in these nonsupercellular squall lines, there might be some other type of special, basically two-dimensional, long-lived cell, or

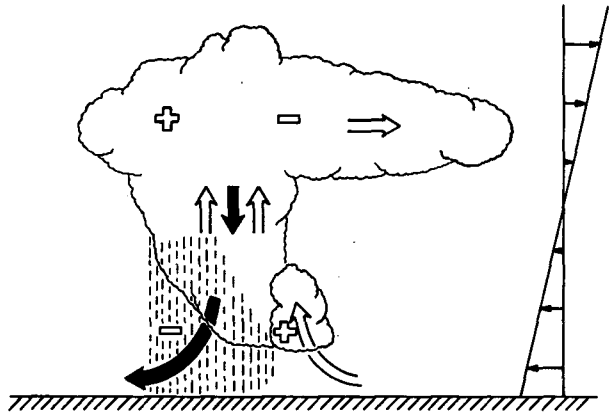

FIG. 2. Newton's proposal that a system of updrafts and downdrafts acts to reduce the shear within the squall line and thus produce a convergence/divergence pattern (indicated by the open plus and minus signs, respectively) which favors new growth downshear of the existing line. (Adapted from Fig. 16 of Newton, 1950.)

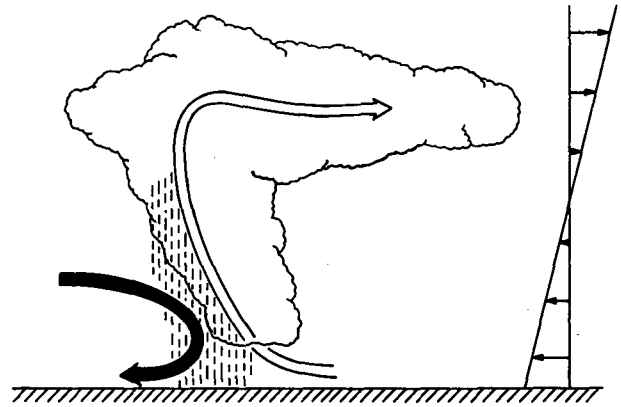

FIG. 3. Ludlam's proposal that a strong updraft leans against the shear and drops its rain out on the upshear side, thus allowing a long-lived cell. (Adapted from Fig. 7d of Ludlam, 1963.)

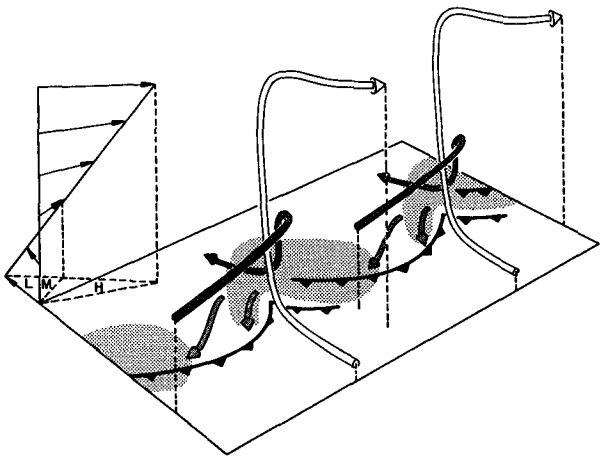

FIG. 4. Lilly's proposal for a line of supercell thunderstorms existing at an angle to the shear so that each supercell could propagate without colliding with a neighbor. The shear profile is indicated on the left; the relative winds at low, middle and high levels are indicated by the L, M and H symbols, respectively. The stippled region indicates the 'hook-shaped' rain area at the surface and the barbed line represents the micro-cold front. (Adapted from Fig. 14 of Lilly, 1979.)

whether one must look instead for conditions which allow for a long-lived, line-oriented system of ordinary short-lived cells as suggested in Newton (1950).

Recently, Thorpe et al. (1982; hereafter TMM) revisited the strictly two-dimensional problem noting that, although the early two-dimensional studies concentrated on environments with deep shear, certain of the studies did report long-lived solutions when the ambient wind profile was either jetlike or one with low-level shear and reduced shear aloft (Takeda, 1971; Hane, 1973). TMM proposed that the long life of the strictly two-dimensional solution is a consequence of the low-level shear in the ambient wind profile. They reasoned that a two-dimensional (no along-line variation) precipitating cell in an environment with no wind shear (Fig. 5a) will have, as in the Byers–Braham picture (Fig. 1b), a rain-produced, surface outflow that moves rapidly away from the cell. However, if the low-level wind relative to the cell (whence the low-level shear) is of sufficient strength, then the outflow may be prevented from moving away from the cell (Fig. 5b). TMM argue (p. 743) that this is a favorable condition for intense, long-lived convection.

TMM's simulated convection has the appearance of a single long-lived cell (see their Fig. 4); we inquire herein whether this sustained two-dimensional solution represents a long-lived cell or a long-lived system of cells. In section 3a, we discuss a two-dimensional simulation conducted under conditions closely resembling those in the TMM study (shear restricted to the lowest 2.5 km directed normal to the squall line) and find, as they did, a long-lived state of intense convection when

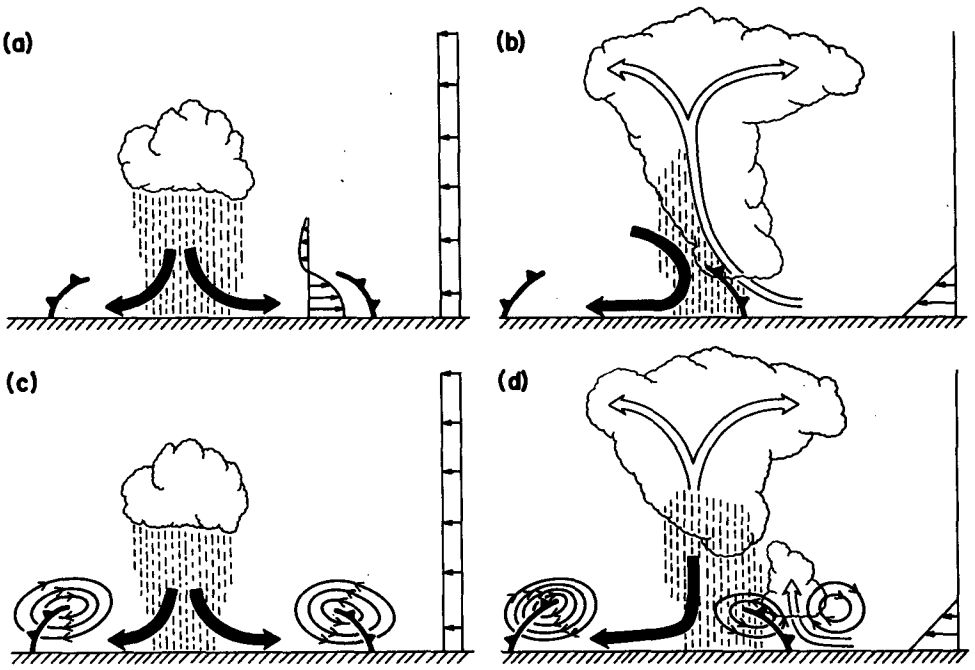

FIG. 5. Thorpe, et al. (1982, pp. 741–743) argue that (a) without low-level shear, the rain-produced cold pool propagates away from the cloud above and that the shear at the top of the pool dissipates new cells triggered by the cold pool, whereas (b) with low-level shear, the cold pool remains beneath the cloud and produces a long-lived cell. In the present study, we argue that (c) without low-level shear, the circulation of a spreading cold pool inhibits deep lifting and so cannot trigger a cell. (d) The presence of low-level shear counteracts the circulation of the cold pool and promotes deep lifting that triggers new cells.

an optimal value is chosen for the low-level shear. In the present case, however, for reasons we will develop below, the long-lived state is characterized by intense convection which is intermittent: a cell will grow and decay, and then its rain-produced cold pool triggers a new cell which repeats the cycle. We present in section 3b the three-dimensional counterpart to these two-dimensional simulations. The three-dimensional simulation shows that the basic balance maintained in the two-dimensional model is also maintained in the three-dimensional counterpart; the individual cells again undergo a repeating cycle of growth and decay, but in this case, they can and do shift their positions along the line. These results establish firmly the nature of the simulated, nonsupercellular squall line as a collection of ordinary time-dependent cells. In section 3c, we report on a three-dimensional simulation with deep, strong (30 m s^{-1} over the lowest 5 km) shear at an angle to the supposed line which produces a line of essentially steady three-dimensional supercells as conjectured by Lilly (1979).

Our interpretation of the nature of the nonsupercellular squall line is the central focus of the present work and is presented in section 4. Past theories of squall-line longevity have emphasized to one degree or another the role of the ambient wind shear, the cold outflow, or some combination of both. We discuss these effects and conclude that the longevity of the intense convection in the nonsupercellular squall line may be explained by the modification of the circulation of the cold outflow due to the presence of low-level ambient shear. We develop herein the idea that without wind shear, a spreading cold outflow induces a circulation in its environment which inhibits deep vertical penetration of the air which it displaces (Fig. 5c). With environmental shear, the cold outflow which tries to spread downshear has its circulation opposed by that of the shear, and consequently, deep penetration may occur (Fig. 5d). With sufficient low-level shear, a new cell is produced at the downshear edge of the cold pool, which was generated by the rainy downdraft of a prior cell. For this reason, we may view the nonsupercellular squall line as a long-lived line of ordinary short-lived cells.

These solutions occur when the shear is sufficient to "balance" the cold pool. In our simulations there is a secular trend in which the cold pool becomes colder over time and so a weaker state eventually develops. This weaker state is characterized by the dominance of the cold-pool circulation which, as described above, inhibits convection. Notwithstanding the weaker cell updrafts, this system continues on for many more hours and assumes a flow structure similar to those observed in highly slanted squall-line circulations with trailing anvils (see the review by Smull and Houze, 1987a).

In the following section, we review the observations of squall-line environments and squall-line circulations. Our approach to the numerical modeling of the squall line is guided by these observations and by the specific theoretical issues discussed. We propose a physical interpretation of the model results in section 4 and discuss the relation of these ideas to observations and other current simulations in section 5. We summarize our findings in section 6.

2. Observations

a. Squall-line environment

Bluestein and Jain (1985), reviewing approximately 10 years of WSR-57 data from the Oklahoma City radar, categorized severe squall lines and computed statistically significant environmental soundings for each of these categories. In addition to the usual finding of large latent instability in the squall-line environment, the grand average hodograph for all cases (Fig. 6a) shows that the largest wind shear is found at low levels with the overall shear vector lying approximately 45° clockwise with respect to the squall line. It should be noted that since Bluestein and Jain restricted their attention to severe cases, their sample contains a number of supercellular squall lines which bias the average hodograph toward the deeper, stronger shear expected for supercells.

Barnes and Sieckman (1984) examined the environmental soundings of tropical mesoscale cloud lines occuring in GATE. They identified two different types of line—fast movers (squall lines) and slow movers. Although much less unstable than its midlatitude counterpart, the environment of the fast mover (Fig. 6b) is also characterized by strong low-level shear (with reversed, weaker shear above 650 mb) and the principal component of the shear is perpendicular to the line. Frank (1978) also concluded that tropical squall lines occur under conditions of relatively strong low-level shear. The environment of the slow mover has virtually zero shear and is more moist above the boundary layer than that of the fast mover.

These studies lend further support to the conclusion from TMM that the low-level shear directed perpendicular to the squall line is the feature of the wind profile that promotes a long-lived system.

b. Squall-line circulation

From the large body of squall-line observations, a consensus emerges on the distribution of equivalent potential temperature, θ_e, in a vertical cross section perpendicular to the squall line. This distribution is reflected by the stippling in the schematic diagrams of Fig. 7. All case studies show that the cumulonimbi, of which the line is composed, are fed by the low-level, high-θ_e air ahead of the line. (By "ahead" and "behind," or "front" and "rear," we will refer to the "downshear" and "upshear" side, with respect to the low-level shear vector, of the active convection depicted in the schematic.) The air behind the line at low levels is cooler

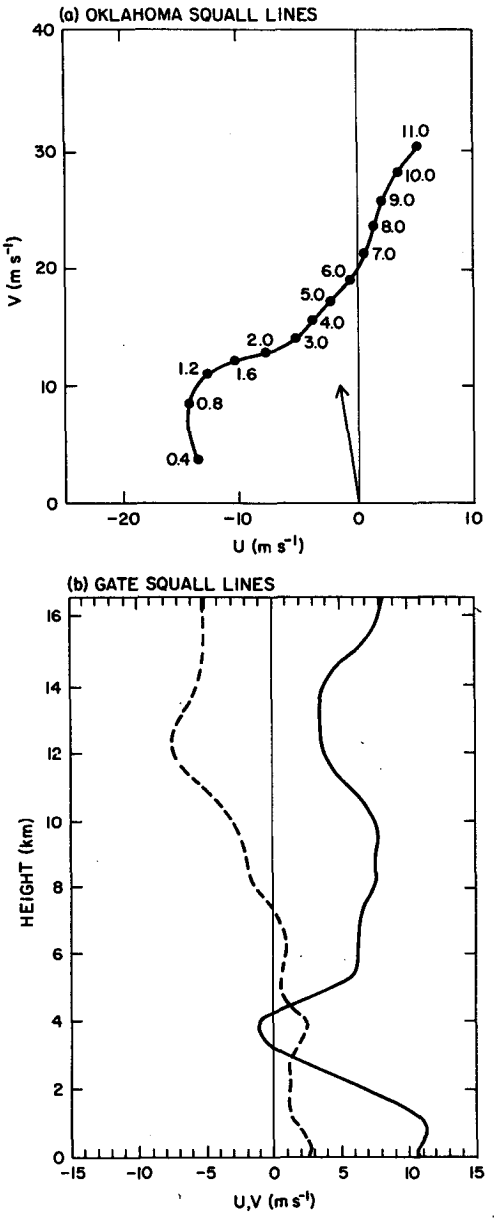

FIG. 6. Characteristic wind profiles for squall lines. (a) An average hodograph for severe squall lines in Oklahoma displaying the cross-line U and along-line V component of the environmental wind (heights labels in km). U is the computed line-relative velocity and the arrow represents the cell motion in this framework (After Bluestein and Jain, 1985) and (b) average line-motion relative across-line wind profile (U, solid) and ground-relative along-line wind profile (V, dashed) for GATE squall lines. (Adapted from Fig. 7 of Barnes and Sieckman, 1984.)

and almost always has lower θ_e than the air ahead; it is far less certain where this air originates. It would exceed the bounds of this study to discuss all published case studies; instead, we offer herein a synthesis of the most prominent studies.

The study by Newton (1963; see Fig. 7b) of the 29 May 1947 squall line, which passed over the Ohio Network of the Thunderstorm Project (Byers and Braham, 1949), is sometimes adduced in support of the Ludlam–Newton model (Fig. 2) in that Newton's two-dimensional streamline plot gives the impression that all the air approaching the line ascends. However, Lilly (1979, p. 157) notes that Newton ". . . did not consider the possibility of substantial three-dimensional motion . . ."; close examination of Newton's Fig. 14 shows there is substantial flow of midlevel low-θ_e air from front to rear which may have been moving between and through the active cumulonimbi and feeding the cold pool behind the line.

The plausibility of this type of three-dimensional flow was established by Zipser (1969) in his study of the structure of a tropical squall line using direct aircraft observations. He found that, in the squall line's mature phase, there is flow from ahead of to behind the line at all levels (see Fig. 7a which is based upon Zipser,

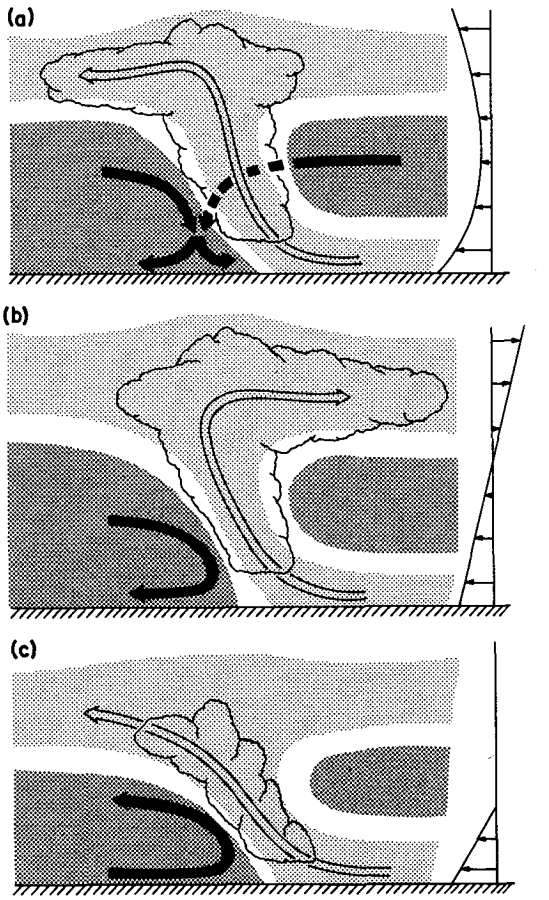

FIG. 7. Schematic diagrams of major conceptual models of squall lines derived from case studies. Lightly and darkly stippled areas indicate areas of high- and low- θ_e air, respectively. (a) Zipser's analysis of a tropical squall line from GATE. (Adapted from Fig. 13 of Zipser, 1977.) (b) Newton's analysis of a squall line from the Thunderstorm Project. (Adapted from Fig. 4 and 14 of Newton, 1963.) (c) Carbone's analysis of a California squall line. (Adapted from Fig. 6 of Carbone, 1982.)

1977; Houze, 1977; Gamache and Houze, 1982). This implies that the low-θ_e air at midlevels ahead of the line must have been moving between and/or through the active cumulus towers. As in the Newton study, Zipser found weak midlevel flow from rear to front behind the line. Recent studies of midlatitude (Smull and Houze, 1985; 1987a; 1987b) and tropical squall lines (Roux et al., 1984; Chong et al., 1987) show that the midlevel front-to-rear flow is intensified in the vicinity of the squall line, and that the flow from rear-to-front behind the line is, in some cases, greater than that found previously.

Zipser's observations also show low-level outflow directed towards the front (indicated in Fig. 7a) and a continually expanding area of low-θ_e air on the rear side of the advancing squall front; the rain-chilled air fills a larger and larger area as the system decays. In fact, most case studies show such a course of events (e.g., see Fujita, 1955, p. 432, Plate IV; Frank, 1978; Leary and Houze, 1979). Some later midlatitude case studies show striking similarities to the tropical cases. For example, Ogura and Liou (1980), in their analysis of the NSSL upper-air mesonetwork soundings through a squall line passing over Oklahoma on 22 May 1976, found flow from front to rear up to 400 mb while, approximately 100 km behind the line, there was midlevel flow from rear to front. They analyzed conventional radar observations and noted that, during the dissipation stage, ". . . the area of high reflectivity (>34 dBZ) in the rear side was separating continuously from the leading edge as time progressed"—indicating to us the expansion of the cold pool noted in the earlier studies. Smull and Houze (1985) noted that this evolution in the reflectivity pattern was accompanied by an increase in the rear-to-front flow. An analysis of another Oklahoma squall line (14 May 1970) by Sanders and Emanuel (1977) exhibits similar behavior in that there was front-to-rear flow up to 400 mb and a clearly defined life-cycle in both cases (see their Fig. 10).

Based on our survey of the data reported in the literature, there seem to be very few features that clearly distinguish midlatitude from tropical squall lines. It is true that tropical squall lines have relative inflow at all levels and so there *must* be "breaks" in the line at some locations. Midlatitude lines have levels which separate flow towards the line from flow away from the line (the so-called *steering level*), but these tend to be at relatively high levels (see Fig. 6a) and it is neither necessary nor likely that all the approaching air between the ground and 6 km overturns and flows away from the line as depicted in Fig. 7b. Instead, as illustrated in Fig. 7a, this air *may* flow through as it *must* in the tropical case. The only important difference between midlatitude and tropical squall lines, in our opinion, is that, because of the more frequent occurrence of deep strong shear with large instability, midlatitude lines might sometimes be composed of three-dimensional supercell storms which may in principle be steady. Indeed, we believe that this type of storm provided the basis for Ludlam's (1963) model which became the archetype for the "midlatitude" squall line.

A recent midlatitude, multi-Doppler analysis (Heymsfield and Schotz, 1985) shows deep front-to-rear flow ahead of the line. Although Heymsfield and Schotz (1985) state that their line did not contain supercells, their Fig. 12 suggests to us that the individual cells may have had supercell-like, three-dimensional circulations. Therefore this case, as well as the recent case reported on by Burgess and Curran (1985) and the earlier cases reported by Newton and Fankhauser (1964), and Browning (1965), may fit Lilly's (1979) line-of-supercells model (Fig. 4) fairly well. In these cases, the environmental shear had a strength and depth consistent with supercell development.

Multi-Doppler analysis of a California (Carbone, 1982) squall line indicates a circulation similar to that shown in Fig. 7c, which resembles that of a "gravity current" (see the laboratory measurements by Britter and Simpson, 1978, in particular their Fig. 10). In Fig. 7c, the location of the *effective* source of the low-θ_e air is to the distant rear behind the line. Carbone's case is interesting since it represents a wintertime squall line in which convection along the squall front may persist in the presense of substantial low-level, cross-line shear, even though there is little or no latent instability of the air ahead of the line (see also, Browning and Harrold, 1970). As we discuss in section 4, we believe the low-level shear alters the gravity-current circulation in a way essential for maintaining the observed convection.

We have been intentionally vague about the horizontal scale in these schematics, as the scales may vary not only from case to case, but within the same case at different times. For example, a close-up view of Fig. 7a in the vicinity of the cold-outflow boundary, would probably bear a strong resemblence to Fig. 7c, with the resemblence increasing as the cold-air outflow increasingly dominates the final stages of the system's life.

In recent years, there has been considerable research on the nature of the trailing region of stratiform precipitation that often forms behind the convectively active portion of squall lines (see the review by Smull and Houze, 1987a). This region is an important aspect of squall lines as a substantial part of the total precipitation produced by the system may occur therein. The numerical simulations conducted in the course of this study indicate that circulations similar to those observed in the trailing-anvil region occur in response to the ongoing convection. Our primary concern in the present paper is with the conditions under which convection will be ongoing and we will discuss overall squall-line structure in the companion paper.

3. Squall-line simulations

We use the cloud model developed by Klemp and Wilhelmson (1978b; hereinafter KW) as our primary

research tool. The premise in the present work, and all antecedent work involving cloud models, is that the squall line's longevity results from a peculiar interaction between cumulus convection and ambient wind shear. Consistent with this premise, we do not examine herein any of the direct effects of earth's rotation. Even with these restrictions, there is still a wide range of parameters, associated with the wind shear and latent instability, that may be varied in a set of numerical experiments. We were guided by the recent climatologies of squall-line environmental soundings from Bluestein and Jain (1985), Barnes and Sieckman (1984), and the modeling work of TMM, and have completed a set of experiments which we will report on in a forthcoming companion paper. In the present study, we look at a subset of these experiments, which, we believe, show most clearly the salient model responses, and which help shed light on the issues discussed in the previous sections.

a. Shallow shear normal to the line: two-dimensional simulation

To perform a reasonably comprehensive set of two- and three-dimensional simulations, we were forced to use fairly coarse resolution. In the present simulation, the model domain extends 180 km in the x direction with a grid interval, $\Delta x = 2$ km. We have verified, with higher-resolution experiments, the importance of the physical mechanisms identified in the coarser-resolution experiments. The domain extends 17.5 km in the vertical with a grid interval, $\Delta z = 700$ m. We use the radiation condition developed by Klemp and Durran (1983) at the upper boundary, and as described by KW, an open boundary condition at the x boundaries and zero-flux-type conditions at the lower surface. No ice processes are included in the present model formulation.

The thermodynamic sounding used for all integrations reported on herein is shown in Fig. 8 and is broadly typical of the environment of midlatitude squall lines (cf. Bluestein and Jain, 1985, their Fig. 17; this sounding is one of those used previously by Weisman and Klemp, 1982, 1984 in their study of the behavior of isolated cells for differing shear and stability profiles). The motion is initiated with a warm (2 K excess) line thermal centered at $x = 90$, $z = 1.4$ km that decays to zero for $|x - 90| > 10$ km and $|z - 1.4| > 1.4$ km as prescribed by Eqs. (4.1) and (4.2) of KW. We have found, in agreement with TMM, that restricting the shear to low levels favors long-lived systems. Also, the climatological evidence suggests that most of the shear perpendicular to the squall line is at low levels (Fig. 6).

We follow TMM and confine a cross-line shear to the lowest 2.5 km: in a series of numerical experiments, we increased the low-level shear from zero to 30 m s^{-1}/2.5 km. For zero shear, no new cells form after the initial cell's rain-produced surface outflow occurs, as

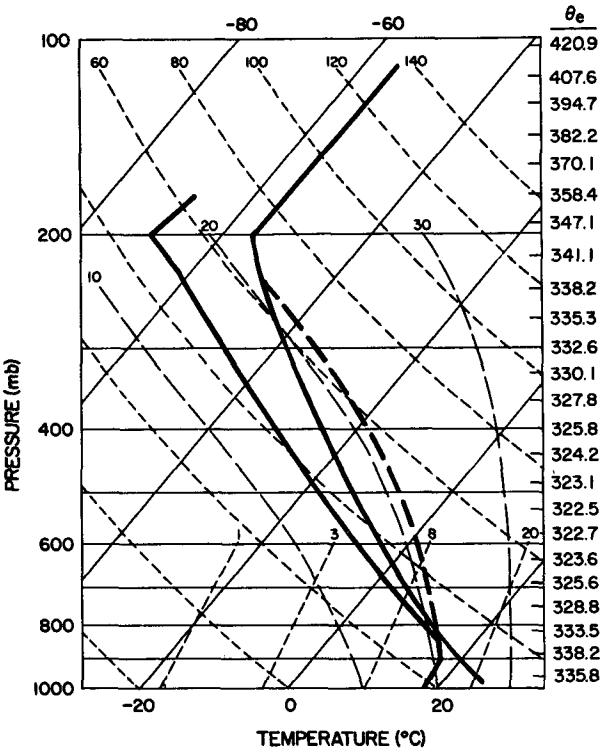

FIG. 8. The thermodynamic sounding used for all simulations presented herein. For ease of reference, we mark the vertical grid levels of the points at which the thermodynamic variables are defined (beginning with $z = 350$ m and increasing by $\Delta z = 700$ m) on the right of the Skew T– Log P chart and list the corresponding values of θ_e.

depicted in Fig. 5a. For slightly larger shear, a new cell forms on the downshear edge of the cold outflow of the original cell. However, further enrichment of the cold pool by the rainy downdraft of this new cell seems to inhibit the penetrative convection characteristic of the initial cell (although condensation of water vapor, release of latent heat and precipitation from the weaker rising motion over the cold outflow continue for a much longer period). Increasing the shear further allows for redevelopment of strong, vertically oriented cells to occur for a longer time before the cold-pool circulation dominates. However, if the shear is too strong, the cell updrafts become much weaker. By trial-and-error we determined that a shear of 17.5 m s^{-1}/2.5 km (Fig. 9) allows for the longest sequence of the strongest cell updrafts. We will emphasize however, that the value of the shear necessary for this state depends crucially on the properties of the cold pool, which, in turn, depend upon the thermodynamic sounding and the nature of the convection produced.

The time series of the maximum vertical velocity, w_{max}, in Fig. 10 provides a broad indicator of the evolving convection in the two-dimensional simulation. The time series indicates the redevelopment of relatively intense updrafts for over 4 h. As discussed, the updrafts over this period take the form of intense, vertically

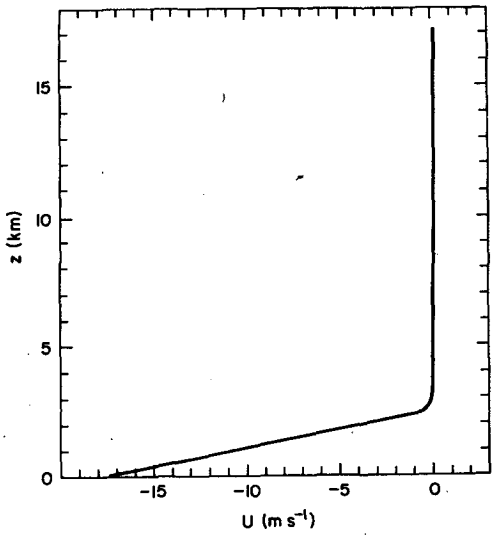

FIG. 9. The wind profile normal to the line used in this study.

penetrating cumulus towers; we refer to this mode as the "optimal state." After 4 h there is a gradual transition to a weaker, less-oscillatory state which lasts as long as the integration is carried out (8 h), and as we shall discuss in section 5a, bears a strong resemblence to squall lines with a trailing region of stratiform precipitation.

Figure 11 depicts the flow as it evolves over the period of one of the oscillations indicated in Fig. 10. Figure 11a shows that the fully developed updraft leans downshear slightly and the accumulated rain falls out of the updraft on the downshear side. The high-θ_e air at the lowest levels flows through the rain "curtain" and becomes cooler and moister (trajectory C). There is also evaporative cooling of the midlevel, low-θ_e air on the downshear side of the updraft which renders the air there negatively buoyant and induces its descent to the ground as shown by trajectory A in Fig. 11b–c. At the surface, both low and high-θ_e parcels (which form a mixture with an intermediate value of θ_e) contribute to the cold pool that triggers a new updraft as illustrated in Fig. 11d (trajectory E). This new updraft subsequently leans downshear and the above-described cycle is repeated; this process continues for a period of approximately four hours. This behavior is very similar to that observed by Sanders and Emanuel (1977; see their Fig. 9). Notice that within this strictly two-dimensional framework, midlevel, front-side air periodically passes to the rear and descends to the surface.

Figure 10b displays a time series of the magnitude of the downdrafts, $w_{\min}$. Near $t = 5$ h there is an intensified downdraft that leads to a significantly colder cold pool (see the time series of $B_{\min}$ in Fig. 10c). Thus begins the transition to the less-ocillatory, weaker mode; Figs. 12a–d display the flow during this period. As the cold pool gets colder, it slowly overcomes the influence of the low-level shear, and begins to surge outward underneath the updraft in the downshear direction. At this stage (Fig. 12a–b), the appearance of the flow is similar to that in the Ludlam–Newton model shown in Fig. 2 and in TMM (see their Fig. 9), evincing, as it does, pronounced "upshear tilt." However, this "upshear tilt" signals the increasing dominance of the cold-pool circulation which leads to less-vigorous further convection. Similar behavior is evident in Fig. 4 of TMM. Although the overall circulation is dominated by the large cold pool, identifiable updraft cells form at the cold-air edge in an unsteady manner and are advected rearward by the cold-pool circulation (Fig. 12d). These weaker cells are minor perturbations on the general circulation, and so are fundamentally different from the unsteady, large-amplitude cells of the optimal state.

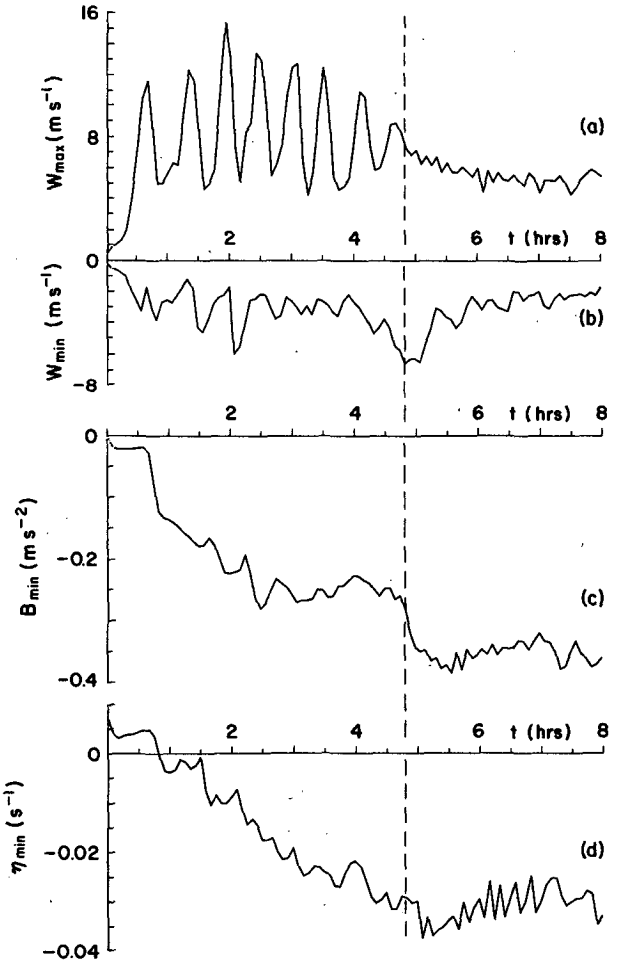

FIG. 10. Time series from the two-dimensional simulation of (a) the maximum vertical velocity, $w_{\max}$, (b) the most intense rainy downdraft velocity, $w_{\min}$, (c) the minimum buoyancy in the cold pool, $B_{\min}$, and (d) the largest negative vorticity associated with the cold-pool edge, $\eta_{\min}$. Note that the quasi-periodic behavior in $w_{\max}$ ends abruptly after an intense downdraft near $t = 5$ h makes the cold pool significantly colder.

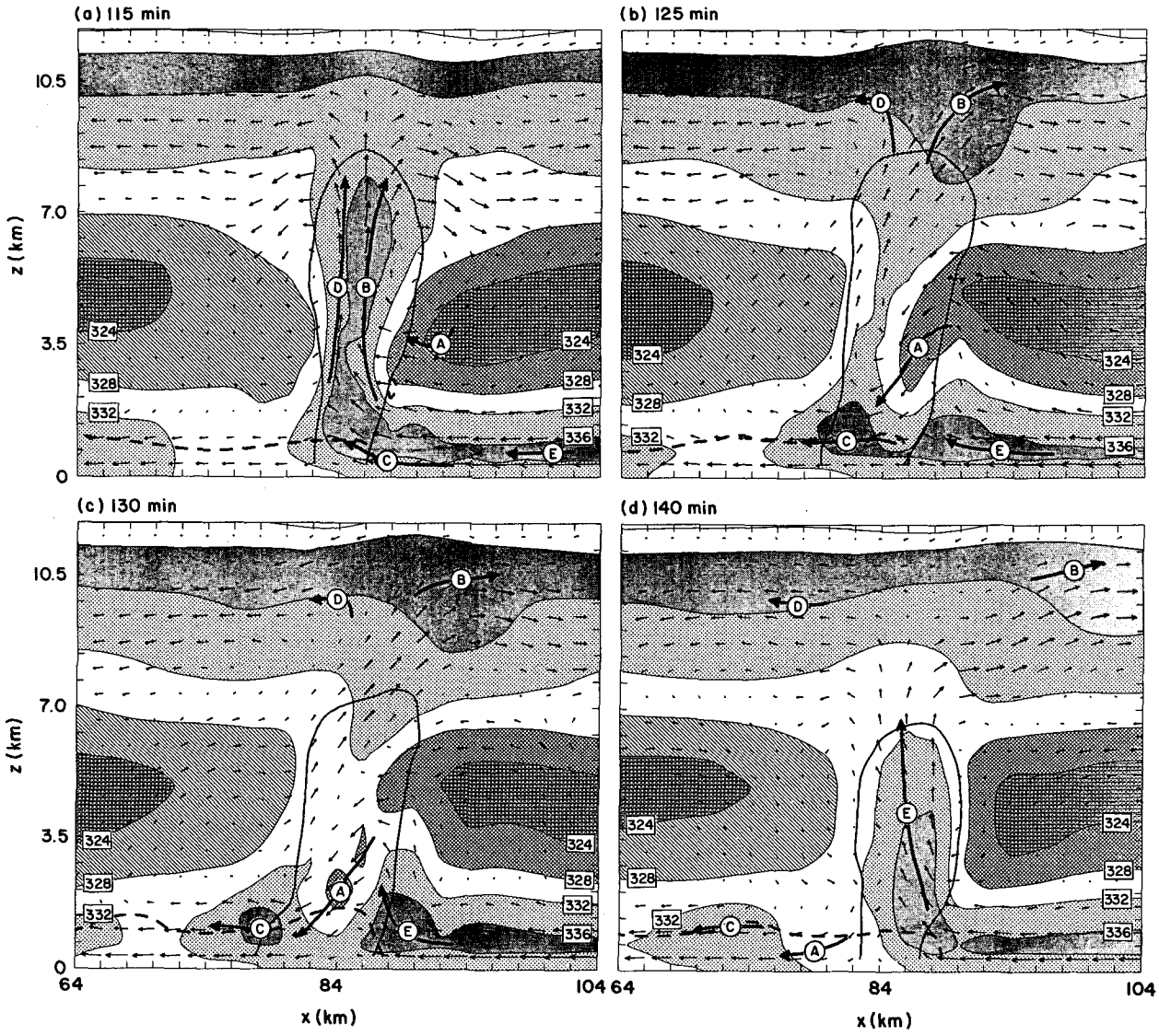

FIG. 11. Time sequence from the two-dimensional simulation showing how one of the oscillating-cell developments occurs. Shown is a portion of the computational domain; the θ_e field is displayed in contour intervals of 4 K which are shaded differentially. The 328–324 interval contains two different shading patterns to distinguish air originating from the front side from that originating from the rear. The thick dashed line is the −1 K perturbation potential temperature contour; the solid line is the 2 g kg^{-1} rainwater countour; the vectors are scaled so that one horizontal grid interval represents 16 m s^{-1}. Selected air-parcel trajectories are followed through the time sequence; at each time, location is indicated by the identifying letter and for 5 min forward and 5 min backward the parcel follows the indicated path. Letters beginning or ending a path signify that the other half of the path was not plotted. (a) t = 115 min. The updraft is fully developed; high-θ_e air is transported upward and it and the rainwater field lean downshear (the parcels D and B originated from the front side earlier). (b) t = 125 min. The downshear leaning rainwater field evaporates into mid- and low-level air on the front side; parcel C flows through the rain and parcel A descends from the front side. (c) t = 130 min. The front-side air from mid- and low levels contribute to the cold pool. (d) t = 140 min. Subsequently a new cell is triggered (parcel E).

The range of variation of $B_{\min}$ is well within the range one would arrive at by hypothesizing slightly different thermodynamic histories of the downdraft air parcels reaching the surface. At one extreme, moist-adiabatic descent of an air parcel from 600 mb to the ground would produce a temperature deficit of −11 K ($B_{\min}$ = −0.36 m s^{-2}) as can be verified from Fig. 8. A combination of moist adiabatic descent from 600 mb to some intermediate level with subsequent dry adiabatic descent to the ground, or moist adiabatic descent from a lower level, easily accounts for the smaller values of $B_{\min}$ shown in Fig. 10c. If the particular time variation of $B_{\min}$ produced in this simulation is a characteristic feature of squall lines, this would support the idea that squall lines could have internally generated life cycles. However, the important general lesson

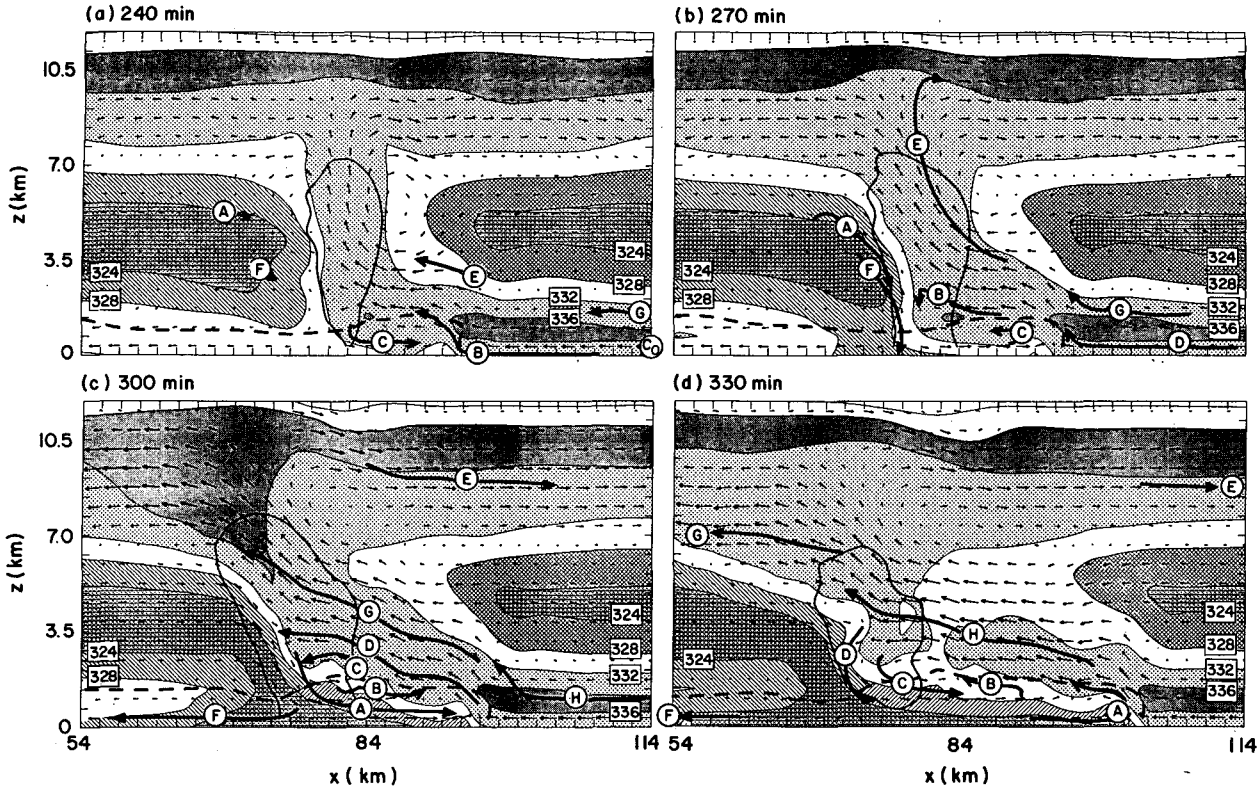

FIG. 12. Time sequence from the two-dimensional model illustrating the phase where the cold pool surges downshear and the system weakens. All descriptors are the same as in Fig. 11 except trajectories extend for 15 min forward and/or backward from the parcel-location indicators. (a) t = 240 min. The cold pool begins to dominate the flow (the parcel C originated from low levels downshear as indicated by the C_0). (b) t = 270 min. Rain evaporates into rear-side midlevel air and induces its descent (parcels A and F). (c) t = 300 min. Rear-side midlevel air pours to the ground. (d) t = 330 min. The cold pool continues to surge downshear as the system weakens. (Note that the cold pool contains both rear- and front-side parcels.)

learned from these simulations is that the lack of a more precise control over the cold pool is, perhaps, the major reason why it is so difficult to maintain an optimal state. The cold pool is generally a result of the convection, and so, the characteristic properties of the cold pool can change substantially depending upon the thermodynamics of the air in the rainy downdrafts.

A related issue is, we believe, that the TMM simulation did not exhibit the quasi-periodic redevelopment observed herein. Our simulations lead us to believe that the strength of TMM's cold pool (introduced initially but subsequently replenished by potentially cold downdrafts) was sufficient to overcome the restraining effect of the imposed shear, and so, their line entered a quasi-steady, weaker mode without evincing an oscillatory phase. To demonstrate that the oscillatory behavior can arise even with a cold-pool initialization, we started the present model with a cold pool of approximately the depth and buoyancy obtained in the simulation during its oscillatory phase. Figure 13 indicates that the oscillatory behavior ensues just as it did after the warm-thermal initiation, thus demonstrating the insensitivity of this mode to the initial perturbation. However, with a shear of 10 m s^{-1} over 2.5 km, there is only one full oscillation before the line enters its weaker mode. Significantly, as we shall emphasize below, convection is not even triggered without

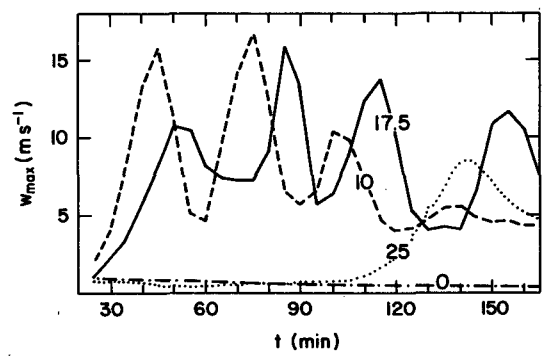

FIG. 13. Time series of maximum vertical velocity from two-dimensional simulations in which convection is initiated with a cold pool instead of a warm thermal. The cold pool is of the temperature and depth of that produced by the precipitating cloud shown in Fig. 11 (minimum potential temperature = −6 K, decreasing linearly to 0 K at z = 1.4 km and extending from x = 0 to x = 90 km). The low-level shear is restricted to the lowest 2.5 km as in Fig. 9, but ΔU varies for each run as indicated.

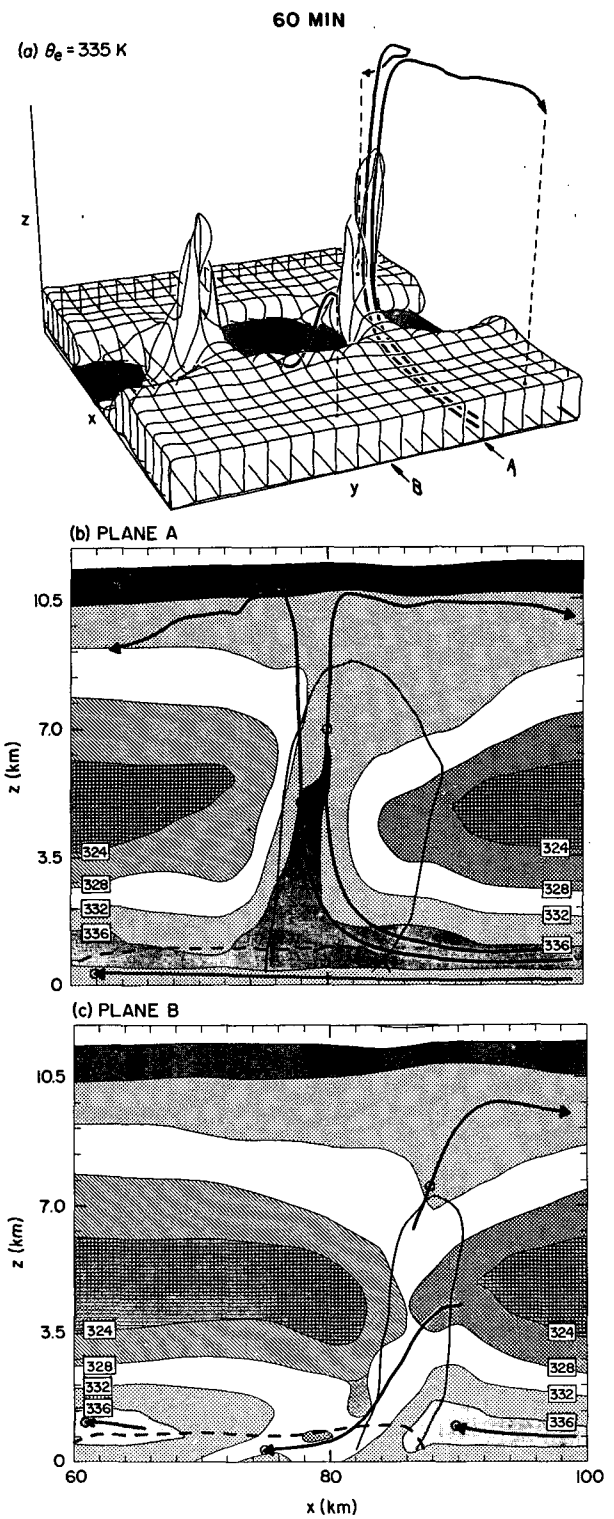

FIG. 14. Three-dimensional counterpart to the two-dimensional simulation (shown Fig. 11) at t = 60 min. (a) A three-dimensional perspective of the θ_e = 335 K surface over a portion of the domain ($60 \leq x \leq 100$ km, $6 \leq y \leq 44$ km) with selected air-parcel trajectories. Shaded regions at the surface show where midlevel, low-θ_e air has scoured out the low-level, high-θ_e air. (b) A view of the flow in an x–z plane through the updraft (Plane A, same trajectories as on three-dimensional plot). (c) A view of the flow through where a downdraft had just occurred (Plane B). All contours indicated as in Figs. 11–12. Small circles indicate where a parcel "pierces" the plane at t = 60 min.

shear, and, with too-strong shear, convection is triggered later, but remains weak.

b. Shallow shear normal to the line: three-dimensional simulation

We construct a three-dimensional counterpart to the two-dimensional simulation by extending the domain 120 km in the y direction with a grid interval, Δy = 2 km and using periodic boundary conditions at the y boundaries. All other conditions are the same as in the two-dimensional simulations except that now small (<0.1 K) random temperature perturbations are superimposed on the initiating line thermal in order to hasten any latent tendency toward three-dimensional motion. Setting periodic boundary conditions in a particular direction obviously puts a strong constraint on the simulated motion. Our philosophy, as in all the earlier two-dimensional model studies, is to circumnavigate the more difficult issues of how and why squall lines begin. We ask only, what orientation and magnitude of shear will allow a given line disturbance to mature into a long-lived system?

This three-dimensional counterpart to the foregoing simulation develops in much the same way, except that with the extra degree of freedom, the line evolves quickly into a line of three-dimensional cells. Figure 14a shows a three-dimensional perspective view at 60 min of the θ_e = 335 K surface along with representative air-parcel trajectories. Figure 14b shows an along-the-shear cross section through the updraft cell (Plane A). As in the two-dimensional simulation, the cell leans downshear and deposits its rain into the oncoming airstream. Figure 14c displays a cross section in a plane through a downdraft (Plane B) which illustrates how the low-θ_e air, ahead of the original cells, descends to the surface forming pools of surface outflow as in the two-dimensional simulation. Updrafts such as the one shown in Fig. 14a, form where the individual pools collide with each other and with the oncoming low-level shear flow (see Droegemeier and Wilhelmson, 1985). This process goes on for several cycles, then, somewhat sooner than in the two-dimensional counterpart, the cold pool becomes colder, surges downshear, and the transition to the weaker, less-oscillatory mode begins.

Figure 15a shows a three-dimensional perspective view of the θ_e = 335 K surface at 160 min, as the downshear-surging of the cold pool is under way. Figure 15b shows an along-the-shear cross section through the updraft cell (Plane A). During this stage, in both the two- and three-dimensional models, the cold-pool air comes from both ahead and behind the line as in the

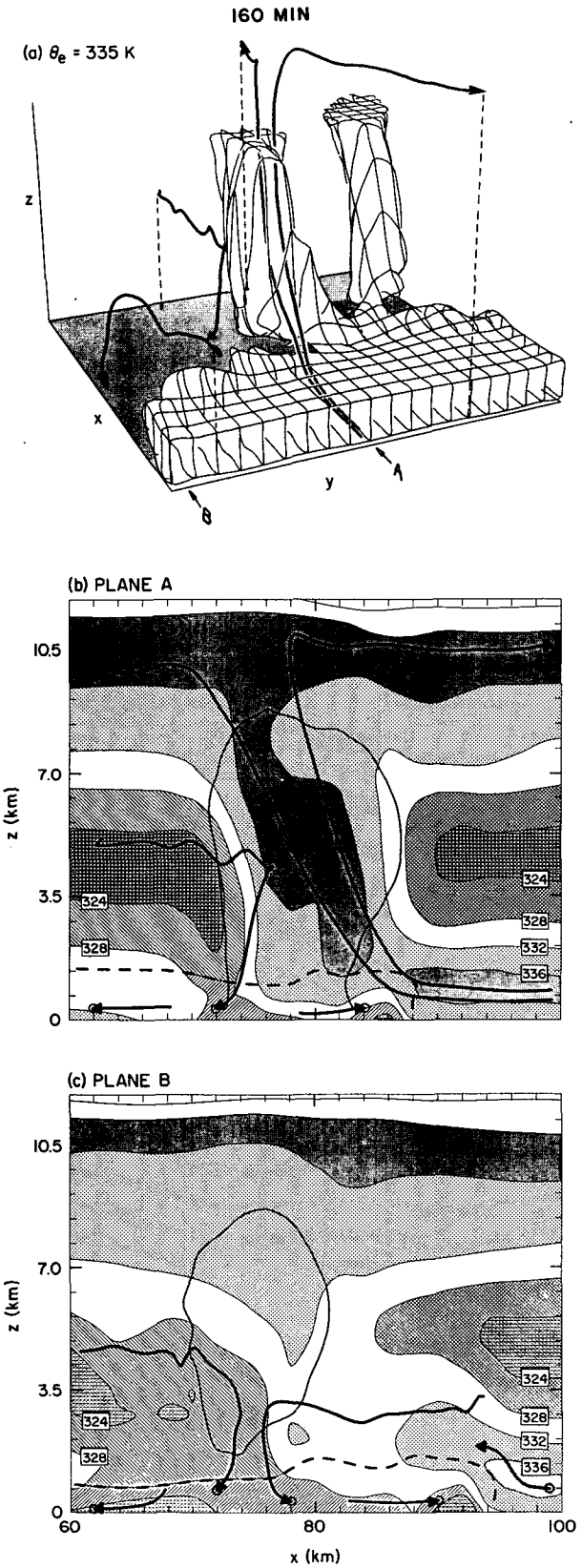

FIG. 15. As in Fig. 14 except at $40 \leq y \leq 78$ km and $t = 160$ min.

Zipser model (Fig. 7a). For this reason we have left the low-level trajectories shown in Figs. 15b–c unconnected to their midlevel origins. Figure 16 contains a map of origins of the cold-pool air parcels at this time which shows that the air in the cold pool is a mixture of front and back-side air.

Although different in detail, we conclude that there is no *essential* difference between the two-and three-dimensional models under the condition of weak-to-moderate low-level shear oriented perpendicular to the squall line. The redevelopment of new cells induced by the interaction of a prior cell's cold surface outflow with the low-level shear is the key mechanism and operates in both two and three dimensions. The three-dimensional solutions begin to depart from their two-dimensional counterparts as the shear is increased further. Under the restriction of two-dimensionality, a weak, nearly steady updraft cell forms whose energy is depleted by the shear (see section 4a); however, in the three-dimensional case, the cells continue to redevelop vigorously since they are relieved of the strong two-dimensional constraint. When the amount of low-level shear is extreme, even the three-dimensional simulations yield weak cells.

c. Deep strong shear at 45° to the line

The midlatitude climatology of Bluestein and Jain (1985) indicates that there is also a significant component of shear along the line (Fig. 6a). With deep, strong, unidirectional shear, three-dimensional cloud models produce updrafts that split, subsequently prop-

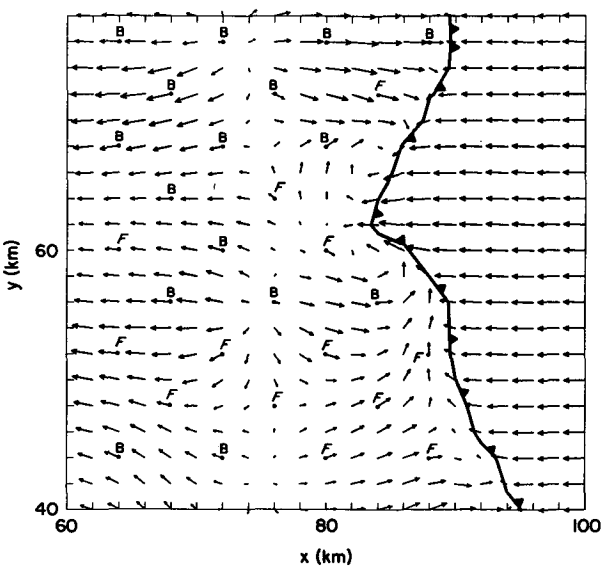

FIG. 16. Map of low-level flow (z = 350 m) corresponding to Fig. 15. One grid interval represents 16 m s^{-1} and the barbed line is the −1 K perturbation potential-temperature contour. The points marked B or F in the cold pool indicate that the air parcels at those points originated either from the back or front side of the line, respectively.

agate transverse to the direction of the shear, and resemble the supercell (e.g., see Rotunno and Klemp, 1985). In the case of shear perpendicular to a line of such storms, the propagating members of the split storm ultimately collide with neighboring split storms and it is impossible to establish a steady cell. If the shear is at an angle to the line, 45° clockwise for example, then, as already mentioned, Lilly (1979, p. 156) conjectures that each cell propagating to the right of the shear remains uninhibited by other cells while the leftward-propagating members move back into the cold air behind the line and decay.

In view of Bluestein and Jain's observations and Lilly's conjecture, we performed experiments orienting the shear at various angles to the direction in which periodicity is imposed. We will report on the full range of these experiments in the companion paper, however, we discuss herein one experiment in which the shear is at a 45° angle to the line, 5 km deep, and 30 m s^{-1}/ 5 km strong. Figure 17 depicts the flow in two of the supercells which form along the direction of periodicity

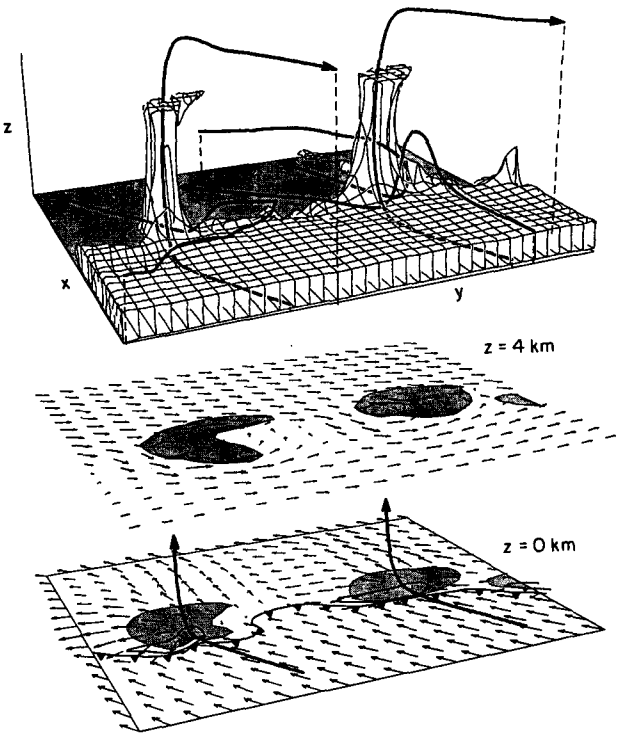

FIG. 17. Top: a three-dimensional perspective view of the θ_e = 335 K surface for a portion ($56 \leq x \leq 116$ km, $14 \leq y \leq 82$ km) of a line containing two supercells. Below there is the z = 4 km horizontal plane exhibiting line-relative flow vectors at every other grid point (a length of two grid intervals = 20 m s^{-1}); the shaded regions encompass places where rainwater exceeds 0.1 g kg^{-1}; the circular contour encompasses updraft greater than 10 m s^{-1}. The flow in the horizontal plane at the surface is denoted similarly except, the updraft contour (at z = 350m) encompasses values greater than 1 m s^{-1} and the barbed line denotes the cold-air boundary defined by the −1 K perturbation.

under these conditions. The perspective view of the θ_e = 335 K surface at t = 170 min is similar in outward appearance to that shown in Fig. 15, except this picture represents a nearly steady state. Also shown is the flow at z = 4 km, which exhibits the rotating updraft characteristic of supercells, and the low-level flow, which exhibits the arc-like gust front, also a property of supercell thunderstorms. The initial line disturbance evolves into a line of supercells which are individually and, owing to their arrangement, collectively steady, and thus represents a type of steady squall line. This experiment also shows that the time-dependence found in the three-dimensional, nonsupercellular squall-line simulations is not an inevitable feature of the present numerical simulations.

4. Interpretation

a. *The role of wind shear*

Early linear theories of convection concluded that wind shear causes updrafts to lean downshear and thus drains them of their energy (Lilly, 1979). Moreover, common thunderstorms were observed to lean downshear and thus to drop their rain into their inflow (Byers and Braham, 1949, p. 101). Thus, shear makes updrafts lean downshear and, for that reason, is detrimental to convection. The observation confuting this conclusion is that some thunderstorms thrive in strong shear (Ludlam, 1963, p. 11). To explain this observation, various investigators set out to explain why, in some circumstances, the wind shear will cause an updraft to lean upshear so that it could feed upon the energy of shear flow and/or drop its rain out of the updraft's inflow stream. (For example, Newton, 1966, argued that the updraft cants against the shear in Ludlam's model because the updraft air tends to conserve the momentum of the lower levels from which it originates.) Contrary to this idea, the foregoing simulations indicate that the tilt of the updraft is not an important factor in determining the longevity of the squall line. Both the two- and three-dimensional simulations discussed in section 3a–b represent a long-lived convective system whose long life is a consequence (as discussed further below) of the shear. However, during the oscillatory phase the updrafts do not tilt upshear with height; later when the intensifying cold pool induces an upshear tilt, the system enters a phase of decidedly weaker convection.

In retrospect, the thunderstorms that motivated the early notion that shear enhances the convection were most likely supercells. Recent studies indicate that ambient wind shear is important to obtain a supercell because the supercell needs shear to rotate, and needs to rotate to sustain its updraft (Rotunno and Klemp, 1985; Weisman and Klemp, 1984). Thus, the tilt of the updraft is not the relevant factor in explaining the supercell's longevity, nor *ipso facto*, the longevity of a squall line composed of supercells.

All numerical models of the present type show that the axis of an initiating thermal/updraft leans downshear. Moncreiff (1978) and Lilly (1985) showed this to be true in particular examples pertaining to deep shear. To clarify why this is true for shallow as well as deep shear, we consider the Boussinesq, inviscid equation governing the component of vorticity directed along a hypothetical line-invariant disturbance, viz.,

$$\rho_0 \frac{d}{dt}\frac{\eta}{\rho_0} = -\frac{\partial B}{\partial x} \tag{1}$$

where

$$\eta \equiv \frac{\partial u}{\partial z} - \frac{\partial w}{\partial x} \tag{2}$$

is the vorticity in the y(along-line)-direction; $\rho_0(z)$, the base-state density; B, the total buoyancy; u, the cross-line velocity; w, the vertical velocity; x, the cross-line distance; z, the altitude; t, the time and d/dt, the rate of change with time following a parcel. Consider the situation illustrated in Fig. 18a: there is at $t = 0$ a warm thermal in a flow with no shear. By the right-hand side of Eq. (1), we see that the buoyancy distribution creates positive vorticity on the right side, and negative on the left side of the thermal, in equal amounts. Thus the axis of the updraft produced by the thermal is vertical. Consider now what happens in a situation with low-level shear as illustrated in Fig. 18c. Let us follow an air parcel up from the boundary layer through the thermal: since the parcel begins with a vorticity, $\eta_0 = dU/dz$, which is positive in our example, a net positive bias develops within the thermally created vortex pair. Therefore, the axis of the updraft, instead of aligning vertically as in the previous no-shear example, now tilts in the downshear direction.

A similar argument obtains for a three-dimensional thermal. The three-dimensional version of Eq. (1) is

$$\rho_0 \frac{d}{dt}\frac{\eta}{\rho_0} = \xi\frac{\partial v}{\partial x} + \eta\frac{\partial v}{\partial y} + \zeta\frac{\partial v}{\partial z} - \frac{\partial B}{\partial x} \tag{3}$$

where v is the along-line velocity and ξ and ζ are the x and z components of the vorticity, respectively. Now consider a columnar thermal; the buoyancy distribution acts as it did before producing positive vorticity on the downshear side and negative on the upshear side, in equal amounts. Again, let's consider a parcel entering the updraft from a low-level shear layer along the centerline ($y = 0$) of the column which, by hypothesis, contains the axis of maximum updraft. By symmetry, the first and third terms on the right-hand side of (3) vanish at $y = 0$; the second term is simply the stretching term in the y direction, which can alter the magnitude but not change the sign of η. Thus an air parcel entering an updraft, as in Fig. 18c, enters with positive η and so again biases the thermally created vortex pair, causing it to lean downshear as in the two-dimensional example. (See also the three-dimensional example from linear theory given by Lilly, 1985.)

We have shown that, in the absence of other influences, columnar updrafts lean downshear; thus either their energy is drained by the shear (unless they are

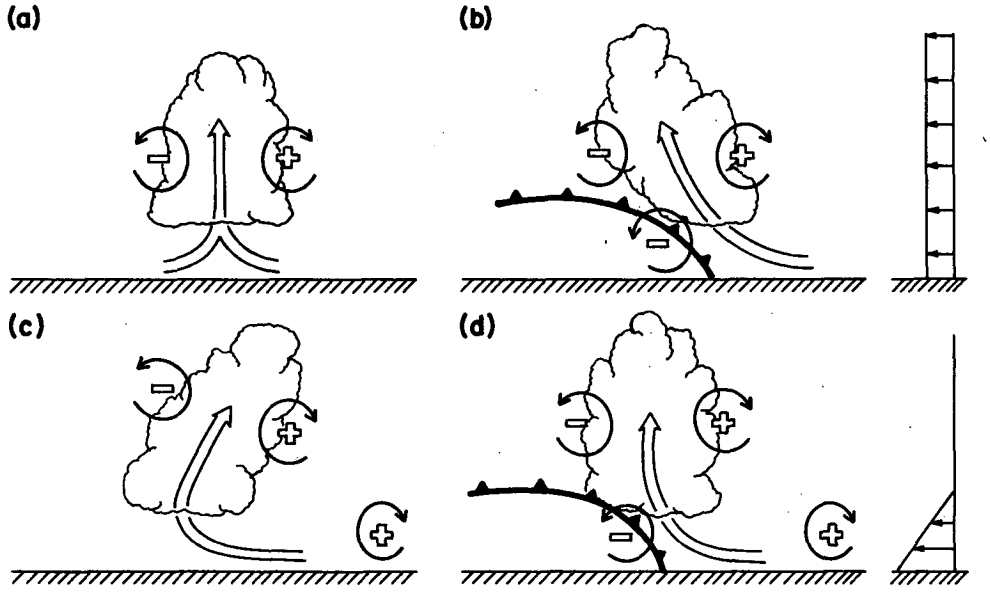

FIG. 18. Schematic diagram showing how a buoyant updraft may be influenced by wind shear and/or a cold pool. (a) With no shear and no cold pool, the axis of the updraft produced by the thermally created, symmetric vorticity distribution is vertical. (b) With a cold pool, the distribution is biased by the negative vorticity of the underlying cold pool and causes the updraft to lean upshear. (c) With shear, the distribution is biased toward positive vorticity and this causes the updraft to lean back over the cold pool. (d) With both a cold pool and shear, the two effects may negate each other, and allow an erect updraft.

supercells) and/or they deposit their rain into their inflow stream. Thus, shear, deep or shallow, acting on either two- or three-dimensional nonsupercellular updrafts is inimical to cumulus convection.

b. *The role of the cold pool*

TMM identified, correctly we believe, the interaction between the surface cold-air pool and the ambient low-level shear as the one that effects the longevity of the squall-line convection. Their explanation for this behavior is that the surface outflow, which issues from the convection aloft, is restrained by the relative subcloud wind. This situates the convergence beneath the cell and thereby prolongs the cell's life. If the subcloud wind is of insufficient strength to restrain the outflow, then, according to TMM (p. 741), the implied shear at the top of the outflow layer (indicated in Fig. 5a) acts to dissipate the convection.

We too noticed that, in experiments with weak low-level shear, the advancing cold front seems to deplete any newly triggered cells of their energy. However, what we found most striking is that, even when the low-level air is lifted above its level of free convection, and above the shear zone at the top of the cold outflow, no new vigorous cells are triggered. Consider, for example, trajectory H in Fig. 12c. This air is as unstable to pseudoadiabatic displacement as any of the preceding parcels which had formed convective cells, such as air-parcel E in Fig. 11. However, Fig. 12 shows that air-parcel H is simply swept rearward by the strong current which develops in response to the downshear-surging cold pool. Parcel H remains well above the shear zone produced at the top of the cold outflow, and so, its lack of convective vigor cannot be attributed to it having had its energy dissipated in that shear zone.

We can understand the difference in behavior between trajectory E and H in terms of the vorticity reasoning used above. Consider the cold pool in a flow with no shear as illustrated in Fig. 18b. As is clear from Eq. (1), negative vorticity is generated at the nose of the cold pool by the buoyancy distribution which defines the cold pool. Air approaching from the right rises and flows toward the rear under the influence of the negative vortex at the edge of the cold pool. In the previous subsection, we argued that wind shear per se is inimical to nonsupercellular updrafts as it causes the updraft to lean downshear. Here we argue that cold outflows per se are also inimical to updrafts as they cause updrafts to lean back over the cold pool. It follows that, shear in the low-level flow (illustrated in Fig. 18d) can change this rearward-directed flow over the cold pool to one in which the approaching flow turns to flow verticially *if the circulation associated with the cold pool's negative vorticity approximately balances the circulation associated with the positive vorticity of the low-level shear.* Since cold pools are located at low levels, the shear can promote convection only when restricted to low levels. We conducted several special experiments with the two-dimensional model in which the shear layer is moved upward. With the shear layer centered at $z = 2.5$ km, the system oscillated only once and then entered its weak-amplitude phase. This indicates that it is the actual shear within the air that makes contact with the cold pool that is influential, not simply the velocity difference between the subcloud and cloud-bearing layer.

c. *The cold pool with and without low-level shear*

To obtain a quantitative criterion for the low-level shear needed to "balance" a cold pool, and to distinguish clearly the physical difference between a cold pool spreading in a no-shear environment from that in an environment with low-level shear, we perform the following analysis. Equation (1) may be written, without further approximation, as

$$\frac{\partial \eta}{\partial t} = -\frac{\partial}{\partial x}(u\eta) - \frac{\partial}{\partial z}(w\eta) - \frac{\partial B}{\partial x}. \tag{4}$$

We fix ourselves in a frame of reference moving with the edge of the cold air and integrate Eq. (4) from a point to the left, $x = L$, to a point to the right, $x = R$, of the cold-air edge, and from the ground to some level, $z = d$, and obtain

$$\underbrace{\frac{\partial}{\partial t}\int_L^R\int_0^d \eta dz dx}_{\text{tendency}} = \underbrace{\int_0^d (u\eta)_L dz}_{\text{flux at left}} - \underbrace{\int_0^d (u\eta)_R dz}_{\text{flux at right}} - \underbrace{\int_L^R (w\eta)_d dx}_{\text{flux at top}} + \underbrace{\int_0^d (B_L - B_R) dz}_{\text{net generation}}. \tag{5}$$

Since we are looking for a steady balance, we set the tendency to zero. Also, in the circumstances investigated herein, there is negligible buoyancy of the air approaching the cold pool, thus we take $B_R = 0$. Finally, we recognize that $\eta \approx \partial u/\partial z$ away from the edge of the cold air. Under these conditions, Eq. (5) becomes

$$0 = \left(\frac{u_{L,d}^2}{2} - \frac{u_{L,0}^2}{2}\right) - \left(\frac{u_{R,d}^2}{2} - \frac{u_{R,0}^2}{2}\right) - \int_L^R (w\eta)_d dx + \int_0^d B_L dz. \tag{6}$$

We consider the situation where the cold air is stagnant (relative to the cold-air edge), so that $u_{L,0} = 0$, and restricted to a height, $z = H$, where $H < d$. With these simplifications, Eq. (6) becomes

$$0 = \frac{u_{L,d}^2}{2} - \left(\frac{u_{R,d}^2}{2} - \frac{u_{R,0}^2}{2}\right) - \int_L^R (w\eta)_d dx + \int_0^H B_L dz. \tag{7}$$

Consider first the case where there is no shear at $x = R$ and a rigid plate at $z = d$. Under these conditions the second and the third terms on the right-hand side of Eq. (7) vanish and we obtain

$$u_{L,d}^2 = 2\int_0^H (-B_L)dz \equiv c^2. \tag{8}$$

If the temperature deficit within the cold pool is a constant, $\Delta\theta$, say, then $-B_L = -g\Delta\theta/\theta_0 \equiv g'$, where θ_0 is the base-state potential temperature. Equation (8) then reduces to

$$u_{L,d}^2 = 2g'H \tag{9}$$

which is identical Benjamin's (1968) Eq. (2.1) (with the acceleration due to gravity, g replaced by g'), and which reduces to the famous von Kármán formula for the speed of a "gravity current" as $d \to \infty$ (since $u_{L,\infty} \to u_R$, and the latter appears in the von Kármán formula). This particular derivation of Eq. (9) from Eq. (5) allows one to interpret the physical situation as one in which *the net buoyant generation of negative vorticity within the volume is just balanced by the export of negative vorticity out the downstream side.*

Now consider a situation where there is low-level shear as illustrated in Fig. 18d. We look for the optimal state where the low-level flow is turned by the cold pool in such a way as to exit as a vertically oriented jet. Thus we set $u_{L,d}$, $u_{R,d}$ and $\int_L^R (w\eta)_d dx = 0$ in Eq. (7) to obtain

$$\Delta u = c, \quad \text{where} \quad \Delta u \equiv u_{R,d} - u_{R,0} = -u_{R,0}. \tag{10}$$

Although this formula is almost identical to Eq. (8), the physical interpretation is fundamentally different. In light of Eq. (5), Eq. (10) states that *the import of the positive vorticity associated with the low-level shear just balances the net buoyant generation of negative vorticity by the cold pool in the volume.*

We illustrate the foregoing ideas by a special set of numerical experiments in which a block of cold air is released in an unstratified environment with a specified low-level shear. Fig. 19 displays a schematic representation of the physical situation and lists the parameters of the numerical simulation. For the cold pool used, Eq. (10) yields $|\Delta u| \approx 20$ m s^{-1}; this should be regarded as a rough guide since the cold pool will try to settle or otherwise be modified by the ambient shear. We look at a small area in the vicinity of the nose of the downshear-moving gravity current (indicated in Fig. 19) at $t = 15$ min, when the flow is nearly steady locally. With no shear (Fig. 20a), the flow is unremarkable inasmuch as it resembles a simple gravity current (see Fig. 10 of Britter and Simpson, 1978). Increasing the shear to 20 m s^{-1}/2 km (Fig. 20b) allows the oncoming air to leave the nose of the pool vertically and rise to 3 km before it turns and flows back toward the right. A further increase in shear to 30 m s^{-1}/2 km (Fig. 20c), shows that oncoming air rises, but to a lesser extent than in the previous case. Figures 20d–f display the vorticity and divergence fields corresponding to the cases shown in Fig. 20a–c. The vorticity is all negative in the case without shear and the convergence (shaded regions) is located at the nose of the cold air at $z = 0$ km and changes to divergence at $z \sim 0.5$ km (Fig. 20d). With increasing low-level shear, the positive vorticity of the shear countervails against the negative vorticity of the cold pool and a deeper (but not stronger) convergence arises (Fig. 20e). However, with too much shear (positive vorticity), the level of zero convergence descends (Fig. 20f). Although the mechanism is different from Newton's (1950, p. 217), our conclusion for the optimal case is the same: "Convergence at the squall front in this [optimal] case occurs throughout a depth of 8–10 000 ft above the surface, rather than in a shallow layer of surface air only."

With this analysis we can understand quantitatively the transition from the quasi-steady oscillatory behavior to the stage where the surging cold pool inhibits convection. Figure 10c displays the time series of $B_{\min}$ in the two-dimensional simulation. Assuming the linear variation within the cold pool, $B_L(z) = B_{\min}(1 - z/H)$, the definition in Eq. (8) gives $c = \sqrt{-B_{\min}H}$.

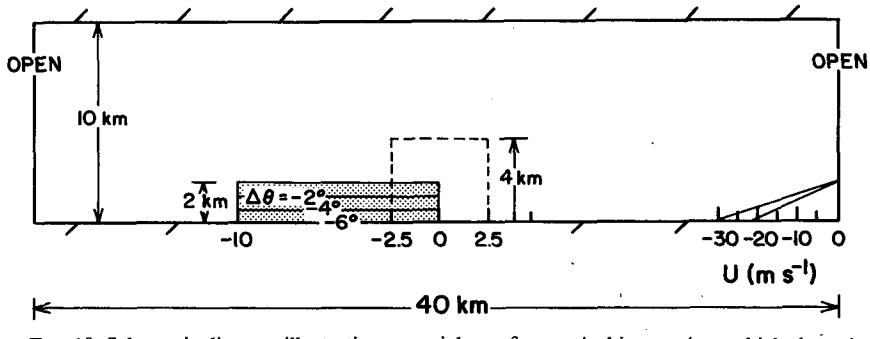

FIG. 19. Schematic diagram illustrating a special set of numerical integrations which show the differing behavior of spreading cold air with a varying amount of low-level shear. The atmosphere is unstratified, the initial cold pool and low-level shear are as specified. The grid resolution in this experiment is $\Delta x = \Delta z = 250$ m. The following figure displays the flow near the downshear edge of the cold pool indicated by the small dashed box.

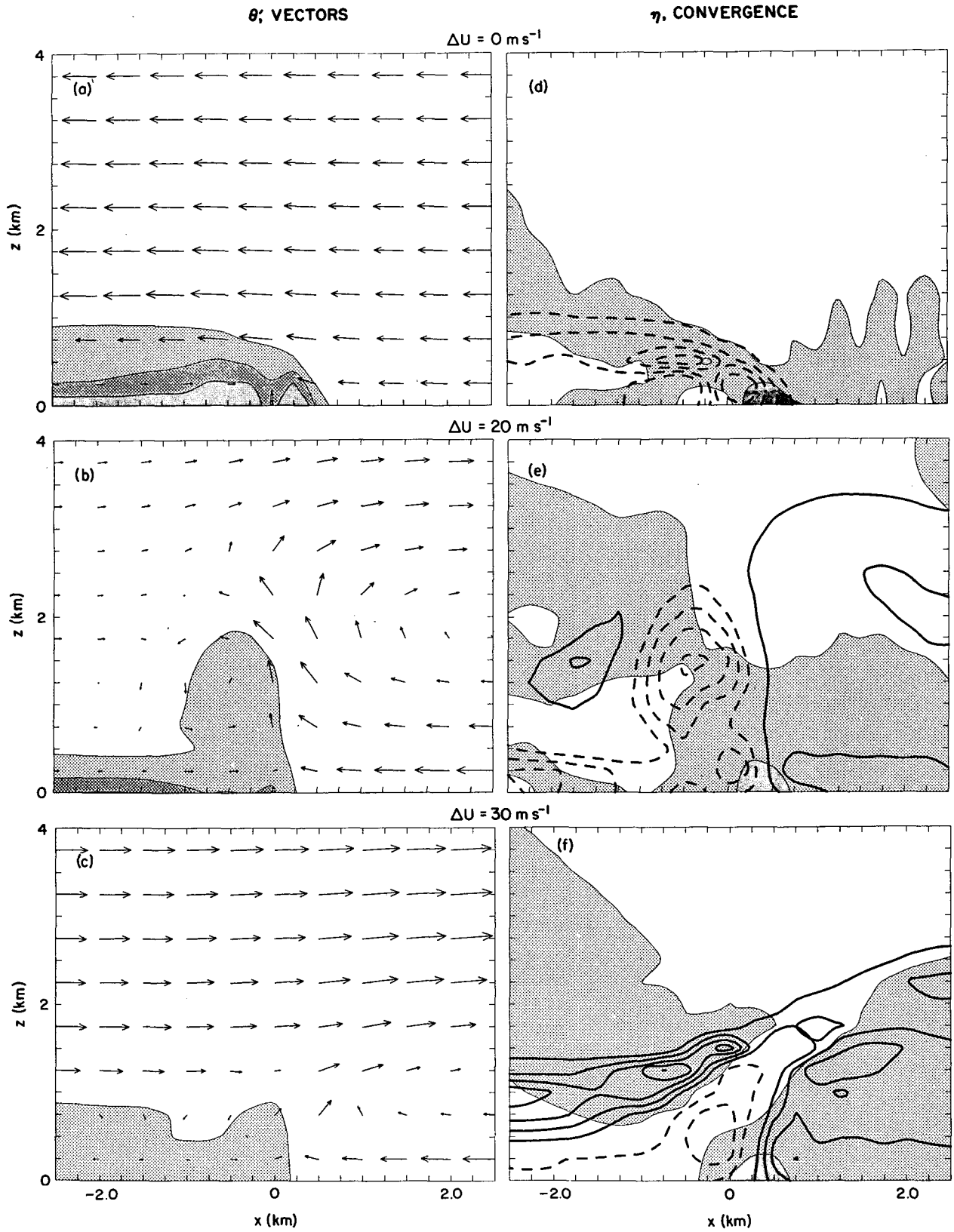

FIG. 20. The spreading cold pool at t = 15 min for ΔU = 0, 20 and 30 m s^{-1}. In (a)–(c), cold pool-relative vectors are plotted at every other grid point (2 grid lengths represents 15 m s^{-1}). The negative potential temperature perturbations are shaded at 2 K intervals, beginning at −1 K. In (d)–(f), η is contoured in intervals of 0.005 s^{-1} (negative values dashed, zero line not shown). Areas of positive convergence are lightly shaded and areas where the convergence exceeds 0.01 s^{-1} are darkly shaded. Convergence is less than 0.016 s^{-1} in all cases.

During the time when the system was quasi-periodic, $-B_{\min} \approx 0.25$ m s^{-2}, and from Fig. 11a, we judge $H \approx 2\Delta z = 1400$ m, thus, $c \approx 18.7$ m s^{-1}; this is close to $\Delta u = 17.5$ m s^{-1} and, according to Eq. (10), the situation is nearly optimal. After the large downdraft intensified near $t = 5$ h (Fig. 10b), the cold pool became deeper and colder; from Fig. 10c, $-B_{\min} \approx 0.35$ m s^{-2}, and from Fig. 12d, $H \approx 2000$ m. With these conditions, $c \approx 26.5$ m s^{-1} indicating a far-from-optimal condition has developed. Figure 10d confirms that the negative vorticity becomes much larger as the transition takes place.

Incidentally, this mechanism of balancing circulations would also explain in fundamental terms why it is so much easier to initiate convection with colliding cold outflows (Droegemeier and Wilhelmson, 1985). Since the two identical colliding outflows necessarily have circulations of opposite sign and equal strength, they induce much deeper lifting of the air they displace than is possible if only one were acting.

d. *Speed of the cold pool*

Equation (10) is a criterion for the ability of a cold pool to generate a vertically erect circulation depending on the low-level shear. If the shear and cold-pool buoyancy are comparable, then we have the optimal case; triggered cells will grow and decay as they move at the speed of the cold pool and this would be the observed speed of a system of time-dependent cells. Since conditions are frequently not optimal, it is desirable to have a formula for the speed of the cold pool in these situations. Although the development of a comprehensive formula is outside the scope of this paper, we can derive an approximate formula using the vorticity balance embodied in Eq. (6) and a few strategic assumptions. We proceed as we did to obtain Eq. (10) except we allow $u_{L,d}$, $u_{R,d}$, $u_{L,0}$ to be nonzero and demand only that, $u_{L,d} = \epsilon u_{R,d}$. The latter condition allows for the propagation of the cold pool with respect to the wind above the shear layer and, for $\epsilon > 1$, the acceleration of the flow in passing over the cold pool; ϵ would be predicted in a more complete theory, but for the present we consider it an external parameter. Under these conditions, Eq. (6) yields

$$\epsilon^2 u_{R,d} = \Delta u - [(1 - \epsilon^2)\Delta u^2 + \epsilon^2(c^2 + u_{L,0}^2)]^{1/2} \quad (11)$$

which recovers Eqs. (8) and (10), respectively, in the appropriate limiting cases.

If the low-level shear is less than optimal, one can show that $u_{R,d} < 0$, and therefore the cold pool propagates faster than the wind above the shear layer. In this less-than-optimal circumstance, triggered cells will again grow and decay (but not as vigorously as in the optimal case), and will be left behind the advancing cold pool. (This is another effect of the less-than-optimal state and not a cause of it.) It is clear that as the system evolves, different features travel at different speeds, and the notion of a system speed becomes much more ambiguous. Our survey of the observational literature indicates that there is wide variation among the many cases studied of a criterion for squall-line motion, including the movement of the centroid of the echo mass, 20 dBZ line, surface wind-shift, etc.

If the low-level shear is greater than optimal, the assumption $u_{L,0} = 0$ would imply that $u_{R,d} > 0$, and in the case of an ordinary cold pool without convection, this is indeed what happens as is evident in Fig. 20c. However with convection, $u_{R,d} > 0$ implies that cells aloft would travel faster than the cold-air edge. This is contradictory since cells drop their rain as they move and thereby define the location of the cold-air edge. In our two-dimensional simulations with stronger-than-optimal low-level shear, the flow is quasi-steady with the low-level flow passing through the rain "curtain" of the (weak) cell aloft and is cooled and slowed in the process. This situation is covered by Eq. (11) by observing that if the cold-air edge moves with the cell aloft, then by definition, $u_{R,d} = 0$; Eq. (11) requires that $u_{L,0} = -\sqrt{\Delta u^2 - c^2}$ which dictates the speed reduction of the air as it passes through the cold-air edge. Consider, for example, that as the cold-pool buoyancy becomes very small ($c \to 0$), the latter expression describes the trivial case of a steady shear flow passing through the volume unchanged. In this strong-shear limit, although the convective system may be steady, the situation is far from optimal since only weak lifting at the cold-air edge is induced.

In case studies and forecasting, ground-relative winds are most frequently used in describing the speed of the system. Based on the foregoing discussion we find the following expressions for the ground-relative cold-pool speed:

$$U_c = \begin{cases} U_{R,0} + c\left[1 - \dfrac{\beta}{2}\left(\dfrac{\Delta u}{c} - 1\right)^2\right], & \Delta u < c \quad (12) \\ U_{R,0} + c, & \Delta u \approx c \quad (13) \\ U_{R,0} + \Delta u, & \Delta u > c \quad (14) \end{cases}$$

where $\beta \equiv \epsilon^2 - 1$ and $U_{R,0}$ is the ground-relative wind to the right of the cold-air edge just above the surface. In deriving Eq. (12), we assumed $u_{L,0} = 0$ (i.e., stagnation behind the cold-air edge) and, for simplicity, $|\beta| \ll 1$; having $\beta > 0$ corresponds to the "finite-depth" effect which acts to reduce the speed of the cold pool as discussed by Benjamin (1968). For the optimal case, Eq. (10) leads directly to Eq. (13), and, Eq. (14) follows directly from the requirement, $u_{R,d} = 0$. From these one may infer that in all cases,

$$\Delta u \leq U_c - U_{R,0} \leq \max(c, \Delta u). \quad (15)$$

Miller and Betts (1977) recognized that the speed of the tropical squall line is the speed of the cold-air pool and used an empirical formula (Simpson and Britter, 1980) to relate that speed to the cold-pool buoyancy

and ambient wind. The present approach may be considered a refinement of that work inasmuch as we have derived an expression for the speed of the cold air from first principles (with β as a parameter). Miller and Betts (1977) do not report $U_{R,0}$ so we cannot make any direct comparison; however, assuming conditions near optimal and light surface winds, Eq. (13) indicates that

$$U_c \approx \alpha\left[\int_0^H (-B_L)dz\right]^{1/2}. \qquad (16)$$

In our analysis, $\alpha = \sqrt{2}$; however, Benjamin (1968, p. 243) conjectures, based on his evaluation of laboratory gravity currents, that the effect of surface friction could lower this to $\alpha \approx 1$, which provides a reasonable fit to the data reported in Fig. 7a of Miller and Betts (1977). (Although this estimate of the speed is a useful result, the criterion for the ability of the cold pool to produce new cells, Eq. 10, is more important; the typical wind profile shown by Miller and Betts suggests the shear was in the optimal range for the reported cases.)

Present and previous numerical cloud models show that the cold pool plays an important role in sustaining deep nonsupercellular convection; moreover, not only the numerical models, but the data show that wind shear is also an important factor. In contradistinction, forced-gravity-wave-type models pertaining to convection in their simplest form (e.g., Lilly, 1979, pp. 142–145) have unstable modes in shearless atmospheres, without any representation of the effects of evaporation, and propagate basically with the speed of an atmospheric gravity wave. Later studies show, however, a strong sensitivity of these modes to ambient shear and heat sinks (Raymond, 1984). For example, in the two-dimensional linear theory of Emanuel (1986), in which the effects of subcloud evaporational cooling (a crude representation of a cold pool) and shear at cloud base are investigated, Emanuel's Fig. 16–17 show, respectively, that as the shear is increased, the downshear-propagating subcloud mode's growth rate increases, and its circulation penetrates more deeply into the atmosphere. Emanuel believes (personal communication) that the vorticity balance described herein accounts for this behavior of this "subcloud mode" as a function of the shear.

Analytic models of steady convective overturning (Moncrieff and Miller, 1976) in their simplest form neglect wind shear, and predict a propagation velocity relative to the surrounding winds which depends on the convective available potential energy (CAPE). In the present numerical experiments, the squall line, in its optimal state, exhibits no significant propagation relative to the winds above the low-level shear layer. Only when the simulated squall line enters the phase where it is dominated by the cold-pool circulation is there upper-level wind relative to the leading edge of the system (by definition). The speed of this type of system is related to the CAPE only in the indirect sense that it is usually necessary to have CAPE to produce the clouds, that produce the rain, that produce the cold pool, that retriggers the cloud, etc. We conducted a special numerical experiment which was identical to the two-dimensional experiment discussed in section 3a, except that the evaporation of rain was not allowed. The initial cell grew as expected since there is large CAPE (indicated in Fig. 8), but it eventually eroded through the usual processes of rain loading and entrainment, and, without the cold pool, no further convection developed. In a further experiment with no evaporation of rain *and* no shear, again, no further convection developed after the initial cell was eroded through rain loading and entrainment.

5. Relation of these ideas to observations

a. The "optimal state"

The foregoing interpretations allow us to be more precise about the definition and significance of the "optimal state." By this we mean a state in which a convective updraft can realize its full CAPE as measured, say, by the positive area on a thermodynamic chart (correcting, of course, for dilution and water loading) without being inhibited by the circulation of either the cold pool or the shear. Put another way, although a cold pool may trigger a cell, the cell can only realize its full potential when the deep circulation of the cold pool, which is detrimental to the cell, is effectively countered by that of the shear. Squall-line convection in this optimal state will be characterized by penetrative convection at the leading edge of the cold pool which a radar would detect as a relatively narrow line of strong reflectivity. Possible examples of this state are: the early behavior of the 22 May 1976 case (see Ogura and Liou, 1980, their Fig. 6a; also Smull and Houze, 1985, their Fig. 3), the "broken-line," "broken-areal" and "embedded-areal" squall-line development of Bluestein and Jain (1985, their Figs. 2, 4–5), the early stages of the tropical squall lines described by Leary and Houze (1979, their Fig. 1a–c) and the one studied by Chong et al. (1987; the early stage shown in their Fig. 7).

A nearly perfect example of a squall line in the "optimal state" is the California squall line analyzed by Carbone (1982). As there was no apparent CAPE in evidence from nearby soundings, it is probable the observed squall-line convection was entirely forced. We suggest that the advance of the cold air in the direction of such a large low-level shear (as was observed) enhanced the convection to a degree which would not have been possible in the absence of such shear. From Carbone's Fig. 18a, we estimate $\Delta u \approx 22$ m s^{-1}, and from his calculation of what is our c (using the factor of 2 in the definition of c), we get $c = 21.4$ m s^{-1}, which is close to optimal.

b. A less-than-optimal shear, but a long-lived state

When the circulation of the cold pool is not countered by a comparable shear, as occurs in the later stages of the present simulation (see Fig. 12), the squall line takes on an entirely different appearance. The rear-to-front flow above the cold pool is intensified (Figs. 12c–d), and the updrafts are weakened (Fig. 10) and the circulation becomes highly slanted. Although the updrafts are weaker, the low-level air lifted over the cold pool continues to rise and produce precipitation over long periods. Also in this stage, there is intensified flow from rear to front behind the line (Figs. 12; follow parcels A and F through the time-sequence). The rear inflow is produced in the present model in reponse to the mass requirements of the cold outflow which spreads in the *upshear* direction; the intensified rear inflow occurs in reponse to the production of a stronger cold pool at $t = 5$ h. This feature will be discussed, along with other aspects of the overall squall-line structure, in the companion paper.

Examples of this less-than-optimal but long-lived state are: the 12 September 1974 GATE case of Gamache and Houze (1982), the later stages of the 22 May 1976 Oklahoma and 10–11 June 1985 Oklahoma–Kansas cases (Smull and Houze, 1985; 1987a; 1987b); the 22 June 1981, West African squall line (Roux et al., 1984; Chong et al., 1987).

Yoshisaki (1986) and Dudhia et al. (1987) have recently reported on two-dimensional numerical simulations pertaining to the GATE and West African cases, respectively. The simulated fields in our Figs. 12c–d are broadly similar to what is obtained in those studies. The only difference of consequence is that the typical ambient wind profile in the environment of tropical squall lines has a layer of reversed shear above the low-level shear. In these jet-profile cases, even if the low-level shear acts to counter the circulation of the cold pool, shear (reversed or otherwise) above the layer containing the cold pool is detrimental to cells which had been triggered below. However, the fact the shear is reversed means that cells will be swept rearward with respect to the cold-air edge, and so, the flow will resemble that in Figs. 12c–d (where the front-to-rear flow develops in response to the increasing dominance of the cold-pool circulation rather than being present in the initial line-relative wind field.)

c. A greater-than-optimal shear, but a long-lived state

When the circulation of the cold pool is too weak for the ambient shear, then the convective system may be long lived but weak. As discussed in section 3, it is the strength of the cold pool *relative* to the low-level shear which to a first approximation determines the strength and longevity of a convective line. To achieve a greater-than-optimal shear for the cold pool produced with the thermodynamic sounding used herein required an unrealistically large low-level shear. As discussed in section 4d, simulations with greater-than-optimal shear exhibited quasi-steady structure with the low-level air passing through a "rain curtain" whereupon it cooled and slowed. The resulting convergence is enough to maintain convection, but the overly strong shear depletes the cells of their convective vigor.

We believe a related finding is one in the study of Dudhia et al. (1987) where their simulated squall line changed from a "multicell" (a highly slanted circulation as descibed above, with periodic pulses of convection moving rearward from the cold-air edge) to a "unicell" (a much steadier single updraft) if the reversed shear aloft is reduced. In light of the analysis in section 4 we offer the following explanation. The sounding for the West African case used by Dudhia et al. (1987, their Fig. 1) is very moist and it would be difficult to produce a cold pool with a temperature deficit much greater than 3 K. In the "multicell" case, the stronger reverse shear leads to a cold pool with $\Delta\theta = -3$ K ($-B_{\min} \approx 0.1$ m s^{-2}) and $H \approx 2$ km, so that $c = \sqrt{-B_{\min}H} \approx 14.1$ m s^{-1} and compares well with the shear between the ground and 2 km, $\Delta u \approx 14$ m s^{-1}. Thus this "multicell" case is nearly optimal but the circulation is highly slanted owing to the reverse shear above the cold pool. (Similar comments apply to the simulation by Yoshizaki, 1986.)

With weaker reverse shear aloft the temperature deficit in the cold air is only $\Delta\theta \approx -1$ K. As explained by Dudhia et al. (1987), the effect of the reduced upper-level shear is to allow rain to fall more or less directly under the cell so that less evaporative cooling occurs. The cold pool, in this case, is too weak to balance the low-level shear and thus nearly steady, but relatively weak, convection persists with low-level air passing directly through the rain curtain, as described in section 4d. We note that the sounding has the potential for a colder cold pool, and speculate that perhaps a different initial condition, or three-dimensionality, would allow this simulation to behave more like the "multicell." As noted by Dudhia et al. (1987) this type of line has yet to be observed.

6. Summary

Using the Klemp–Wilhelmson cloud model, we have attempted to understand the factors that allow a line-oriented disturbance to mature into a long-lived system of precipitating cumulus convection. We find two basic types of simulated long-lived squall lines: lines of more-or-less ordinary cells that continually grow and decay, and lines of nearly steady supercells. The former occurs under conditions of strong shear at low levels directed perpendicular to the line, with weak shear aloft. The latter occurs with strong, deep shear at an angle to the line, which allows the three-dimensional circulation within each cell to persist without interference from its neighbors.

The observations discussed in section 2 suggest that the most common mode of squall line is one with un-

steady cells growing and decaying along a line oriented perpendicular to a strong low-level shear. The airflow patterns within midlatitude and tropical squall lines do not appear to be fundamentally different; they are basically unsteady and three-dimensional, as illustrated in Fig. 7a. In fact, all of the airflow patterns shown in Fig. 7 are observed in a single simulation in which a squall line evolves through a complete life cycle. In the two- and three-dimensional experiments with shallow shear, the flow was from front to rear in the early stages similar to that illustrated by the two arrows approaching the convection in Fig. 7a. At later stages, a flow from rear-to-front develops behind the convective region and the simulations strongly resembles the schematic in Fig. 7b, although as we have noted, the circulation progressively leans further upshear as the cold pool dominates the circulation. As the cold pool fills a larger and larger area, the leading edge of the spreading pool will give rise to the gravity-current-like circulation depicted in Fig. 7c. However, the simulations show that the cold pool continues to be fed by midlevel air originating on both the front and rear sides of the line and, thus the overall flow most nearly resembles Fig. 7a.

The essential ingredient that sustains a long-lived line of time-dependent cells is an amount of low-level shear which counters the circulation induced by the cold thunderstorm outflow. As illustrated in Fig. 18c, in the absence of a cold pool, an updraft/thermal will tilt downshear. As precipitation reaches the surface, evaporation produces a cold pool which triggers a new cell (Fig. 18d). This triggering, and subsequent growth, of the new cell depends crucially on the shear profile. Droegemeier (1985) first found in numerical simulations that cold pools produce deeper lifting when there is low-level shear. Recent theoretical and laboratory studies (Rottman et al., 1985; Jirka and Arita, 1987) demonstrate that ambient shear alters the circulation at the leading edge of a cold pool in a manner consistent with that described herein. Our analysis of the physics (section 4c) provides a new interpretation of the von Kármán formula and explains how the low-level shear alters fundamentally the basic gravity-current circulation to one which provides a more propitious environment for growing cells. The propensity for convective initiation along the intersections of colliding outflow boundaries may also be explained by this same process of deep lifting produced by the balancing of oppositely oriented low-level circulations.

These solutions occur for an optimal value of windshear magnitude in comparison to the depth and coldness of the outflow. When the shear is less than optimal for a given cold pool, the simulated squall-line circulation is highly slanted and has weak updrafts. Referring back to our argument, with shear too weak for a given cold pool, the outflow from a prior cell induces a circulation above it that inhibits convection and leads to the weaker state. In our simulations, there is a secular trend in which the cold pool becomes colder over time. Since the low-level shear feeding the convection changes only slightly with time, a less-than-optimal state eventually develops in which the cold pool's circulation makes it progressively more difficult for new cells to form and the system ultimately changes to the weaker state. We believe this is the state simulated in TMM, and in recent simulations of tropical squall lines.

The observations show that lines composed of supercell-like circulations occur, but far less frequently. The airflow in the supercell is as depicted in Browning's (1964) well-known schematic of interlocking up- and downdrafts. The airflow in a line of supercells is simply a concatenation of many of these steady circulations aligned so as to minimize their mutual interference as shown in Fig. 4. The simulated line of supercells shown in Fig. 17 is such a collection of individually steady, three-dimensional cells. Rotunno and Klemp (1985) have shown that the major reason these simulated supercells propagate is because the updraft's rotation always induces new updraft growth on its right flank; lifting at the nose of the cold pool is thus relegated to a relatively minor role in the supercell. Since this mechanism requires the continued existence of the updraft to produce new updraft on the right flank, the supercell is more properly viewed as steady and, therefore, a squall line composed of such cells is *ipso facto* steady.

In principle, one can evaluate whether or not atmospheric conditions would favor the evolution of long-lived squall lines. From a thermodynamic sounding one can estimate c (e.g., see Betts and Silva Dias, 1979), and from a wind profile sounding, one can estimate Δu. If these two quantities are comparable, then according to Eq. (10), the balance between the cold-pool circulation and the low-level shear is nearly optimal. The greatest uncertainty in this evaluation lies in estimating the strength and depth of the cold pool since these features are a product of the convection and may be sensitive to the details of its evolution. At present, we view Eqs. (10)–(14) primarily as diagnostic relationships that support our interpretation of the important squall-line dynamics.

We have demonstrated that in the presence of wind shear the flow in the vicinity of a cold pool may differ substantially from that which occurs in a traditional gravity current. When the environment is stratified, the moving cold pool produces internal gravity waves which further alter its behavior. The nature of spreading cold pools in these more varied conditions found in the atmosphere is currently being investigated by Klemp and Rotunno.

The observations also showed a number of cases that don't fit easily within the *weltansicht* of squall lines offered herein. Srivastava et al. (1986) observed a squall line which redeveloped far ahead of the cold outflows of the squall line thunderstorms. This may be due to larger-scale effects as this system occured under conditions of strong synoptic-scale forcing. The slow-

moving cloud lines mentioned in section 2a may or may not differ qualitatively from the squall lines discussed above. Although the slow-moving lines have very little cross-line shear, the cold pool is also extremely weak (see the Appendix of Barnes and Sieckman, 1984); hence it is possible that the slow mover fits within the general view developed herein. On the other hand, the slow movement over the warm tropical ocean suggests that surface energy transfer may play an important role, or the generally weak convective motions themselves might be more greatly affected by internal gravity waves in the free atmosphere. These phenomena all await convincing explanation.

Acknowledgments. We have benefited greatly from innumerable conversations with Drs. G. Barnes, H. Bluestein, K. Emanuel, D. Lilly, M. LeMone, T. Matejka, D. Parsons, D. Raymond, A. Thorpe, and E. Zipser.

REFERENCES

Barnes, G. M., and K. Sieckman, 1984: The environment of fast- and slow-moving tropical mesoscale convective cloud lines. *Mon. Wea. Rev.*, **112,** 1782–1794.

Benjamin, T. B., 1968: Gravity currents and related phenomena. *J. Fluid Mech.*, **31,** 209–248.

Betts A. K., and M. F. Silva Dias, 1979: Unsaturated downdraft thermodynamics in cumulonimbus. *J. Atmos. Sci.*, **36,** 1061–1071.

Bluestein, H. B., and M. H. Jain, 1985: Formation of mesoscale lines of precipitation: severe squall lines in Oklahoma during the spring. *J. Atmos. Sci.*, **42,** 1711–1732.

Britter, R. E., and J. E. Simpson, 1978: Experiments on the dynamics of a gravity current head. *J. Fluid Mech.*, **88,** 223–240.

Browning, K. A., 1964: Airflow and precipitation trajectories within severe local storms which travel to the right of the mean wind. *J. Atmos. Sci.*, **21,** 634–639.

——, 1965: Some inferences about the updraft within a severe local storm. *J. Atmos. Sci.*, **22,** 669–677.

——, and F. H. Ludlam, 1962: Airflow in convective storms. *Quart. J. Roy. Meteor. Soc.*, **88,** 117–135.

——, and T. W. Harrold, 1970: Air motion and precipitation growth at a cold front. *Quart. J. Roy. Meteor. Soc.*, **96,** 369–389.

Burgess, D. W., and E. B. Curran, 1985: The relationship of storm type to environment in Oklahoma on 26 April 1984. *Preprints 14th Conf. on Severe Local Storms*, Amer. Meteor. Soc., Boston, MA 02108, 208–211.

Byers, H. R., and R. R. Braham, 1949: *The Thunderstorm.* U. S. Gov't Printing Office, Washington DC, 287 pp. [NTIS PB-234-515.]

Carbone, R. E., 1982: A severe frontal rainband. Part I: stormwide hydrodynamic structure. *J. Atmos. Sci.*, **39,** 258–279.

Chong, M., P. Amayenc, G. Scialom and J. Testud, 1987: A tropical squall line observed during the COPT 81 experiment in West Africa. Part 1: kinematic structure inferred from dual-Doppler radar data. *Mon. Wea. Rev.*, **115,** 670–694.

Droegemeier, K. K., 1985: The numerical simulation of thunderstorm outflow dynamics. Ph.D. thesis. University of Illinois at Urbana-Champagne, 695pp. [Available from University Microfilms, Ann Arbor, MI, Order No. AAD86-00166.]

——, and R. B. Wilhelmson, 1985: Three-dimensional numerical modeling of convection produced by interacting thunderstorm outflows. Part I: control simulation and low-level moisture variations. *J. Atmos. Sci.*, **42,** 2381–2403.

Dudhia, J., M. W. Moncrieff and D. K. W. So, 1987: The two-dimensional dynamics of West African squall lines. *Quart. J. Roy. Meteor. Soc.*, **113,** 121–146.

Emanuel, K. A., 1986: Some dynamical aspects of precipitating convection. *J. Atmos. Sci.*, **43,** 2183–2198.

Frank, W. M., 1978: The life cycles of GATE convective systems. *J. Atmos. Sci.*, **35,** 1256–1264.

Fujita, T., 1955: Results of detailed synoptic studies of squall lines. *Tellus*, **7,** 405–436.

Gamache, J. F., and R. A. Houze, Jr., 1982: Mesoscale air motions associated with a tropical squall line. *Mon. Wea. Rev.*, **110,** 118–135.

Glossary of Meteorology, R. E. Huschke, Ed., 1959. Amer. Meteor. Soc., Boston, p. 534.

Hane, C. E., 1973: The squall line thunderstorm: numerical experimentation. *J. Atmos. Sci.*, **30,** 1672–1690.

Heymsfield, G. M., and S. Schotz, 1985: Structure and evolution of a severe squall line over Oklahoma. *Mon. Wea. Rev.*, **113,** 1563–1589.

Houze, R. A., 1977: Structure and dynamics of a tropical squall-line system. *Mon. Wea. Rev.*, **105,** 1540–1567.

Jirka, G. H., and M. Arita, 1987: Density currents or density wedges: boundary-layer influence and control methods. *J. Fluid Mech.*, **177,** 187–206.

Klemp, J. B., and R. B. Wilhelmson, 1978a: Simulations of right- and left- moving storms produced through storm splitting. *J. Atmos. Sci.*, **35,** 1097–1110.

—— and ——, 1978b: The simulation of three-dimensional convective storm dynamics. *J. Atmos. Sci.*, **35,** 1070–1096.

——, and D. R. Durran, 1983: An upper boundary condition permitting internal gravity wave radiation in numerical mesoscale models. *Mon. Wea. Rev.*, **111,** 430–444.

Leary, C. A., and R. A. Houze, 1979: The structure and evolution of convection in a tropical cloud cluster. *J. Atmos. Sci.*, **36,** 437–457.

Lilly, D. K., 1979: The dynamical structure and evolution of thunderstorms and squall lines. *Ann. Rev. Earth Planet. Sci.*, **7,** 117–171.

——, 1985: The structure, energetics and propagation of rotating convective storms. Part I: energy exchange with the mean flow. *J. Atmos. Sci.*, **43,** 113–125.

Ludlam, F. H., 1963: Severe local storms: a review. *Meteor. Monogr.*, **5,** Amer. Meteor. Soc. 1–30.

Miller, M. J., and A. K. Betts, 1977: Traveling convective storms over Venezuela. *Mon. Wea. Rev.*, **105,** 833–838.

Moncrieff, M. W., 1978: The dynamical structure of two-dimensional steady convection in constant vertical shear. *Quart. J. Roy. Meteor. Soc.*, **104,** 543–567.

——, and M. J. Miller, 1976: The dynamics and simulation of tropical cumulonimbus and squall lines. *Quart. J. Roy. Meteor. Soc.*, **102,** 373–394.

Newton, C. W., 1950: Structure and mechanism of the prefrontal squall line. *J. Meteor.*, **7,** 210–222.

——, 1963: Dynamics of severe convective storms. *Meteor. Monogr.*, **5,** Amer. Meteor. Soc. 33–58.

——, 1966: Circulations in large sheared cumulonimbus. *Tellus*, **18,** 699–713.

——, and J. C. Fankhauser, 1964: On the movements of convective storms, with emphasis on size discrimination in relation to water-budget requirements. *J. Appl. Meteor.*, **3,** 651–668.

Ogura, Y., and M.-T. Liou, 1980: The structure of a midlatitude squall line: a case study. *J. Atmos. Sci.*, **37,** 553–567.

Raymond, D. J., 1984: A wave-CISK model of squall lines. *J. Atmos. Sci.*, **41,** 1946–1958.

Rottman, J. W., J. C. R. Hunt and A. Mercer, 1985: The initial and gravity-spreading phases of heavy gas dispersion: comparison of models with phase I data. *J. Hazardous Materials*, **11,** 261–279.

Rotunno, R., and J. B. Klemp, 1985: On the rotation and propagation of simulated supercell thunderstorms. *J. Atmos. Sci.*, **42,** 271–292.

Roux, F., J. Testud, M. Payen and B. Pinty, 1984: West African squall-line thermodynamic structure retrieved from dual-Doppler radar observations. *J. Atmos. Sci.*, **41,** 3104–3121.

Simpson, J. E., and R. E. Britter, 1980: A laboratory model of an

atmospheric mesofront. *Quart. J. Roy. Meteor. Soc.*, **106,** 485–500.

Smull, B. F., and R. A. Houze, Jr., 1985: A midlatitute squall line with a trailing region of stratiform rain: radar and satellite observations. *Mon. Wea. Rev.*, **113,** 117–133.

——, and ——, 1987a: Rear Inflow in squall lines with trailing stratiform precipitation. *Mon. Wea. Rev.*, (in press)

——, and ——, 1987b: Dual-Doppler radar analysis of a midlatitude squall line with a trailing region of stratiform rain. *J. Atmos. Sci.*, (in press)

Sanders, F., and K. A. Emanuel, 1977: The momentum budget and temporal evolution of a mesoscale convective system. *J. Atmos. Sci.*, **34,** 322–330.

Srivastava, R. C., T. J. Matejka and T. J. Lorello, 1986: Doppler radar study of the trailing anvil region associated with a squall line. *J. Atmos. Sci.*, **43,** 356–377.

Takeda, T., 1971: Numerical simulation of a precipitating convective cloud: the formation of a "long-lasting" cloud. *J. Atmos. Sci.*, **28,** 350–375.

Thorpe, A. J., M. J. Miller and M. W. Moncrieff, 1982: Two-dimensional convection in nonconstant shear: a model of midlatitude squall lines. *Quart. J. Roy. Meteor. Soc.*, **108,** 739–762.

Weisman, M. L., and J. B. Klemp, 1982: The dependence of numerically simulated convective storms on wind shear and buoyancy. *Mon. Wea. Rev.*, **110,** 504–520.

——, and ——, 1984: The structure and classification of numerically simulated convective storms in directionally varying wind shears. *Mon. Wea. Rev.*, **112,** 2479–2498.

Wilhelmson R. B., and J. B. Klemp, 1983: Numerical simulations of severe storms within lines. *Preprints 13th Conf. on Severe Local Storms*, Amer. Meteor. Soc., Boston, 231–234.

Yoshizaki, M., 1986: Numerical simulations of tropical squall-line clusters: two-dimensional model. *J. Meteor. Soc. Japan*, **64,** 469–491.

Zipser, E. J., 1969: The role of organized unsaturated downdrafts in the structure and rapid decay of an equatorial disturbance. *J. Appl. Meteor.*, **8,** 799–814.

——, 1977: Mesoscale and convective-scale downdrafts as distinct components of squall-line structure. *Mon. Wea. Rev.*, **105,** 1568–1589.